EUROPEAN ORGANIZATION FOR PARTICLE PHYSICS

LEPEWWG/96-01
ALEPH 96-043 PHYSIC 96-039
DELPHI 96-36 PHYS 609
L3 Note 1927
OPAL Technical Note TN 360
SLD Physics Note 47
29 March 1996

A Combination of Preliminary LEP and SLD Electroweak Measurements and Constraints on the Standard Model

The LEP Electroweak Working Group*
and the SLD Heavy Flavor Group†.

Internal Note

Prepared from Contributions of the LEP and SLD Experiments to the 1996 winter conferences.

Abstract

This note presents a combination of published and preliminary electroweak results from the four LEP collaborations and the SLD collaboration which were prepared for the 1996 winter conferences. Averages of the results concerning electroweak physics are presented. They are derived from the measurements of hadronic and leptonic cross sections, the leptonic forward-backward asymmetries, the τ polarization asymmetries, the $b\overline{b}$ and $c\overline{c}$ partial widths and forward-backward asymmetries and the $q\overline{q}$ charge asymmetry. The main differences with respect to the results presented at the 95 summer conferences are the updated measurements of the $c\overline{c}$ partial width, the τ polarization asymmetries and of the $q\overline{q}$ charge asymmetry. The results are compared to precise electroweak measurements from other experiments. The parameters of the Standard Model are evaluated, first using the combined LEP electroweak measurements, and then using the full set of precise electroweak results.

*The present members of the LEP Electroweak Working Group are D. Abbaneo, P. Antilogus, T. Behnke, D. Bloch, A. Blondel, G. Borisov, I. Brock, D.G. Charlton, R. Clare, P. Clarke, S. Dutta, S. Ganguli, M.W. Grünewald, A. Gurtu, K. Hamacher, M. Hildreth, R.W.L. Jones, A. Kunin, L. Malgeri, M. Martinez, F. Matorras, M.-N. Minard, K. Mönig, A. Olshevsky, Ch. Paus, M. Pepe-Altarelli, P. Perret, D. Piccolo, B. Pietrzyk, G. Quast, P. Renton, D. Reid, M. Roney, D. Schaile, D. Schlatter, T.J. Smith, R. Tenchini, F. Teubert, and P.S. Wells.

†The representatives of the SLD Heavy Flavor group are E. Etion, B. Schumm and D. Su.

1 Introduction

In a recent note [1] the four LEP experiments have presented parameters derived from the Z resonance using published and preliminary results based on data recorded until the end of 1994. The preliminary results were contributions to the 1995 International Europhysics Conference on High-Energy Physics, 27/7 to 2/8/1995, Brussels, Belgium and the 17th International Symposium on Lepton-Photon Interactions, 10-15/8/1995, Beijing, China.

Since then several additional preliminary analyses have become available. In addition, there are a few preliminary results from the 1995 Z scan. Results from the the high energy (130–140 GeV) run at the end of 1995 are presented elsewhere [2].

The data consist of the hadronic and leptonic cross sections, the leptonic forward-backward asymmetries, the τ polarization asymmetries, the $\mathrm{b\overline{b}}$ and $\mathrm{c\overline{c}}$ partial widths and forward-backward asymmetries and the $\mathrm{q\overline{q}}$ charge asymmetry. Many technical aspects of their combination have already been described in References 3, 4 and references therein. It should be stressed, however, that several measurements included in the current combination are still preliminary.

This note is organized in the following manner. In Section 2 the results on the Z line shape and leptonic forward-backward asymmetries are presented, while Section 3 contains the measurements of the τ polarization. Section 4 describes the parameters resulting from heavy flavour analyses, Section 5 new results for the inclusive hadronic charge asymmetry. Section 6 is devoted to the interpretation of the results. In Sections 6.1, 6.2 and 6.3 several LEP electroweak measurements are combined to determine the effective neutral current coupling constants and to give a value of the effective electroweak mixing angle. We also quote values for these parameters when the left-right and left-right forward-backward asymmetries from SLD [5–7] are included. The determination of the number of light neutrino species is discussed in Section 6.4. In Section 6.5 the LEP data and also data from SLD [5–8], from neutrino interactions [9–11] and from measurements of the mass of the W boson [12–15] and the top quark [16, 17] are used to constrain the parameters of the Standard Model.

2 Z Lineshape and Lepton Forward-Backward Asymmetries

The results presented here are based on the data taken during the energy scans in 1990 and 1991 with centre-of-mass energies, $\sqrt{s}$, in a range $|\sqrt{s} - m_{\mathrm{Z}}| < 3$ GeV, on the data collected at the Z peak in 1992 and on a preliminary analyses of the energy scan in 1993 and the peak running in 1994. Two experiments include preliminary results on the lepton forward-backward asymmetries using data from the 1995 energy scan where each experiment collected approximately 40 pb^{-1} at and near the Z peak.

The total statistics and the systematic errors on the individual analyses of the four LEP collaborations are given in Tables 1 and 2. Details of the individual analyses can be found in References 18–21.

During the 1995 data-taking period it was discovered, using newly installed measurement probes, that the dipole field in the LEP magnets drifts during a physics fill. These drifts are caused by parasitic currents generated by electrically powered trains in the Geneva area. While it is clear that similar drifts had to be present in the past, the current status of the analysis does not yet allow a quantitative statement. For the results presented here, we use a 10 MeV error for the 1995 center-of-mass energies, while the energies and errors for earlier years are the ones used in Reference 1. A discussion of the implications of a change in the LEP energy scale, and thus a change in m_{Z} and possibly Γ_{Z} is presented in section 6.5.

For the averaging of results the LEP experiments provide a standard set of 9 parameters describing the information contained in hadronic and leptonic cross sections and leptonic forward-backward asymmetries [3, 22]. These parameters have initial-state QED corrections, as well as t-channel and s/t-interference contributions in the case of the e^+e^- final state, removed. They are convenient for fitting and averaging since they have small correlations. The parameters are:

- The mass and total width of the Z boson, where the definition is based on the Breit-Wigner denominator $(s - m_Z^2 + is\Gamma_Z/m_Z)$ [23].
- The hadronic pole cross section of Z exchange:

$$\sigma_h^0 \equiv \frac{12\pi}{m_Z^2}\frac{\Gamma_{ee}\Gamma_{had}}{\Gamma_Z^2}.$$

  Here Γ_{ee} and Γ_{had} are the partial widths of the Z for decays into electrons and hadrons.

- The ratios:

$$R_e \equiv \Gamma_{had}/\Gamma_{ee} \quad R_\mu \equiv \Gamma_{had}/\Gamma_{\mu\mu} \quad R_\tau \equiv \Gamma_{had}/\Gamma_{\tau\tau}. \tag{1}$$

  Here $\Gamma_{\mu\mu}$ and $\Gamma_{\tau\tau}$ are the partial widths of the Z for the decays $Z \to \mu^+\mu^-$ and $Z \to \tau^+\tau^-$. Even under the assumption of lepton universality a small difference of 0.2% is expected between the values for R_e and R_μ, and the value for R_τ, owing to mass corrections to $\Gamma_{\tau\tau}$.

- The pole asymmetries, $A_{FB}^{0,e}$, $A_{FB}^{0,\mu}$ and $A_{FB}^{0,\tau}$ for the processes $e^+e^- \to e^+e^-$, $e^+e^- \to \mu^+\mu^-$ and $e^+e^- \to \tau^+\tau^-$. In terms of the effective vector and axial-vector neutral current couplings of fermions, g_{Vf} and g_{Af}, the pole asymmetries are expressed as:[1]

$$A_{FB}^{0,f} \equiv \frac{3}{4}\mathcal{A}_e\mathcal{A}_f \tag{2}$$

  with:

$$\mathcal{A}_f \equiv \frac{2g_{Vf}g_{Af}}{g_{Vf}^2 + g_{Af}^2}. \tag{3}$$

This set of 9 parameters does not describe the Z production and decay completely, because it does not include the interference of the Z exchange with the γ exchange. This contribution is investigated in a separate note [2]. For the results presented in this Section, the γ-exchange contributions and the γZ interference terms are fixed to their Standard Model values.[2]

The four sets of 9 parameters provided by the LEP experiments are presented in Table 3. The covariance matrix of these parameters is as described in our previous paper [22]. It is constructed from the covariance matrices of the individual LEP experiments and common systematic errors. These common errors arise from the theoretical uncertainty in the luminosity normalization affecting the hadronic pole cross section, $\Delta\sigma_h^0/\sigma_h^0 = 0.16\%$, from the uncertainty of the LEP centre-of-mass energy spread of 5 MeV [24], resulting in $\Delta\Gamma_Z \approx 1.0$ MeV, and from the uncertainty in the LEP energy calibration. The latter uncertainty causes errors of $\Delta m_Z \approx 1.5$ MeV, $\Delta\Gamma_Z \approx 1.7$ MeV, and $\Delta A_{FB}^{0,\ell} \approx 0.0005$ for each lepton species ($\ell = e, \mu, \tau$). Full correlation between $A_{FB}^{0,\mu}$ and $A_{FB}^{0,\tau}$ and full anti-correlation between $A_{FB}^{0,e}$ and $A_{FB}^{0,\mu}$ or $A_{FB}^{0,\tau}$ is used. This anti-correlation for $A_{FB}^{0,e}$ is an approximation

[1] In the definition of $A_{FB}^{0,f}$, effects coming from γ exchange, γ/Z interference, as well as real and imaginary parts of the photon vacuum polarization are not included. They are accounted for explicitly in the fitting formulae used by the experiments, and are fixed to their Standard Model values.

[2] If instead the γZ interference terms are entirely determined from LEP cross-section data (including the 130-140 GeV data), the total error on the LEP average of m_Z increases from 2.2 MeV to 4.8 MeV [2].

of the effect of the t-channel contribution for a typical LEP experimental acceptance for the e^+e^- final state. The combined parameter set and its correlation matrix are given in Tables 4 and 5.

If lepton universality is assumed, the set of 9 parameters given above is reduced to a set of 5 parameters. R_ℓ is defined as $R_\ell \equiv \Gamma_{\rm had}/\Gamma_{\ell\ell}$, where $\Gamma_{\ell\ell}$ refers to the partial Z width for the decay into a pair of massless charged leptons.

The data of each of the four LEP experiments are consistent with lepton universality (the difference in χ^2 over the difference in d.o.f. with and without the assumption of lepton universality are 6/4, 4/4, 4/4 and 5/4 for ALEPH, DELPHI, L3 and OPAL, respectively). Based on this assumption Table 6 provides the five parameters $m_{\rm Z}$, $\Gamma_{\rm Z}$, $\sigma^0_{\rm h}$, R_ℓ and $A^{0,\ell}_{\rm FB}$ for the individual LEP experiments. The four experiments all use the above definition of $\Gamma_{\ell\ell}$. Tables 7 and 8 provide these five parameters and the corresponding correlation matrix for the combined result of the four LEP experiments. Figure 1 shows, for each lepton species and for the combination assuming lepton universality, the resulting 68% probability contours in the R_ℓ-$A^{0,\ell}_{\rm FB}$ plane.

For completeness the partial decay widths of the Z boson are listed in Table 9.

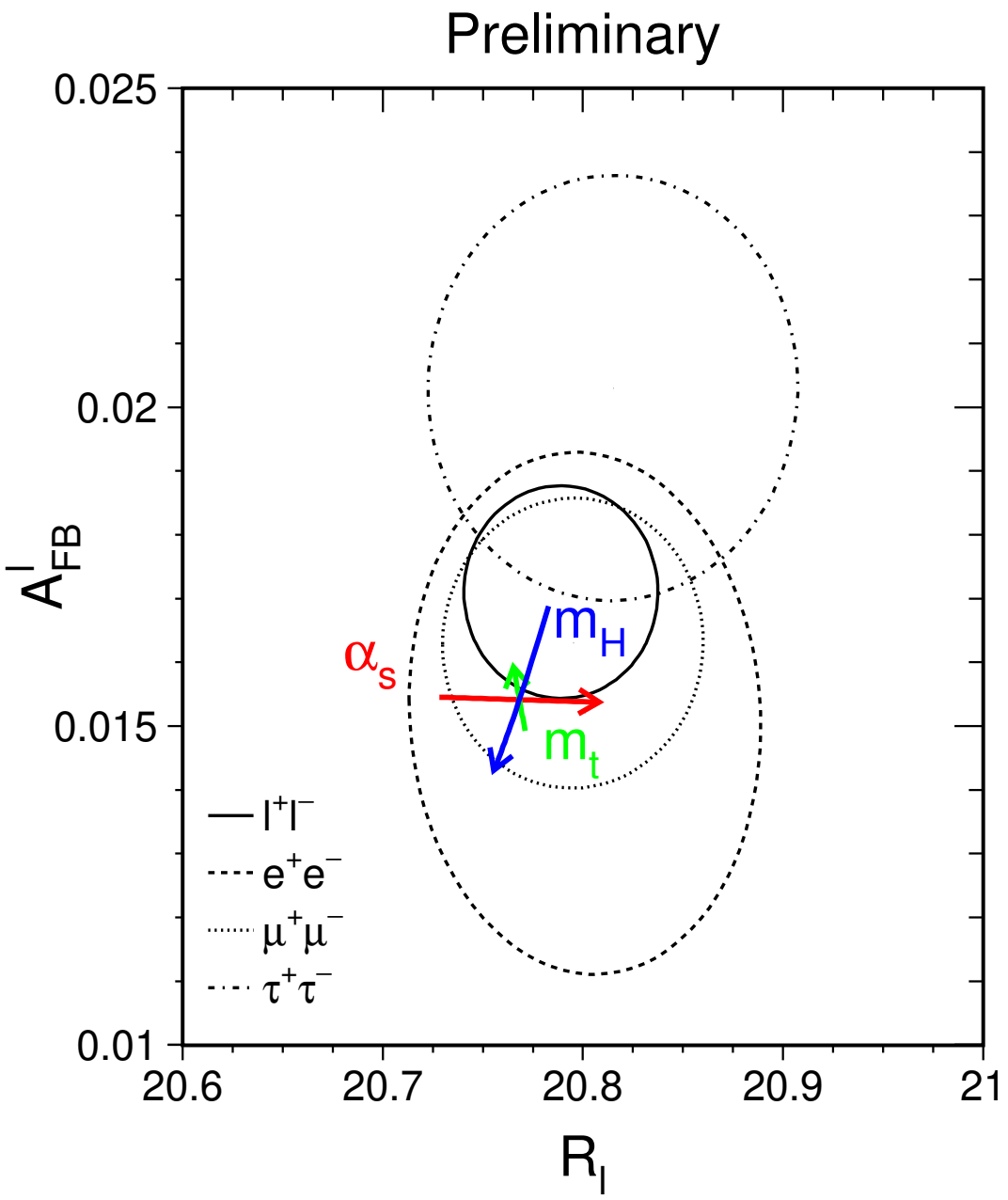

Figure 1: Contours of 68% probability in the R_ℓ-$A_{\rm FB}^{0,\ell}$ plane. The Standard Model prediction for $m_{\rm Z} = 91.1884$ GeV, $m_{\rm t} = 175$ GeV, $m_{\rm H} = 300$ GeV, and $\alpha_s = 0.123$ is also shown. The lines with arrows correspond to the variation of the Standard Model prediction when $m_{\rm t}$, $m_{\rm H}$ or $\alpha_s(m_{\rm Z}^2)$ are varied in the intervals $m_{\rm t} = 175 \pm 9$ GeV, $m_{\rm H} = 300^{+700}_{-240}$ GeV, and $\alpha_s(m_{\rm Z}^2) = 0.123 \pm 0.006$, respectively. The arrows point in the direction of increasing values of $m_{\rm t}$, $m_{\rm H}$ and α_s.

		ALEPH	DELPHI	L3	OPAL	LEP
$q\bar{q}$	'90-'91	451	356	416	454	1677
	'92	680	697	678	733	2788
	'93 prel.	640	677	654	646	2617
	'94 prel.	1281	1144	1362	1524	5311
	total	3052	2874	3110	3357	12393
$\ell^+\ell^-$	'90-'91	55	37	40	58	190
	'92	82	69	58	88	297
	'93 prel.	78	71	61	82	292
	'94 prel.	[a]155	124	123	184	586
	'95 prel.	[c] 55	[b]22	–	–	77
	total	425	323	282	412	1442

Table 1: The LEP statistics in units of 10^3 events used for the analysis of the Z line shape and lepton forward-backward asymmetries.
[a]Statistics used in the measurement of the lepton cross section. The statistics used in the lepton forward-backward asymmetries is about 27% higher.
[b]The results for leptons are for the e^+e^- and $\mu^+\mu^-$ channels only.
[c]The results for leptons are for the $\mu^+\mu^-$ and $\tau^+\tau^-$ channels only.

	ALEPH			DELPHI			L3		OPAL	
	'93 prel.	'94 prel.	'95 prel.	'93 prel.	'94 prel.	'95 prel.	'93 prel.	'94 prel.	'93 prel.	'94 prel.
$\mathcal{L}^{\text{exp.}}$ ([])	0.087%	0.116%	[a]	0.21%	0.09%	[a]	0.12%	0.15%	0.076%	0.079%
σ_{had}	0.073%	0.073%	[a]	0.13%	0.15%	[a]	0.08%	0.2%	0.15%	0.16%
σ_{e}	0.50 %	0.48%	[a]	0.44%	[a]	[a]	0.3%	0.4%	0.23%	0.24%
σ_{μ}	0.25 %	0.26%	[a]	0.28%	0.40%	[a]	0.3%	0.6%	0.16%	0.15%
σ_{τ}	0.34 %	0.32%	[a]	0.8%	[a]	[a]	0.6%	1.5%	0.43%	0.46%
A_{FB}^{e}	0.003	0.003	[a]	0.0026	0.0025	0.0055	0.004	0.004	0.0016	0.0016
A_{FB}^{μ}	0.001	0.001	0.001	0.0009	0.0015	0.0025	0.001	0.002	0.001	0.001
A_{FB}^{τ}	0.004	0.004	0.001	0.0023	0.0030	[a]	0.004	0.006	0.002	0.002

Table 2: The experimental systematic errors for the analysis of the Z line shape and lepton forward-backward asymmetries at the Z peak. The errors quoted do not include the common uncertainty due to the LEP energy calibration. The treatment of correlations between the errors for different years is described in References 18–21.
[a]No preliminary result quoted yet.
[b]In addition, there is a theoretical error for the calculation of the small angle Bhabha cross section of 0.16%, which has been treated as common to all experiments. The DELPHI theoretical error for 1993 is 0.17%.

	ALEPH	DELPHI	L3	OPAL
$m_{\rm Z}$(GeV)	91.1921±0.0037	91.1849±0.0034	91.1936±0.0036	91.1852±0.0036
$\Gamma_{\rm Z}$(GeV)	2.4955±0.0055	2.4914±0.0053	2.5022±0.0054	2.4960±0.0053
$\sigma^0_{\rm h}$(nb)	41.55±0.09	41.40±0.10	41.48±0.11	41.47±0.10
R_e	20.54±0.11	20.90±0.16	20.89±0.12	20.90±0.10
R_μ	20.88±0.09	20.69±0.09	20.80±0.11	20.796±0.073
R_τ	20.77±0.10	20.62±0.16	20.73±0.17	21.00±0.11
$A^{0,\rm e}_{\rm FB}$	0.0195±0.0044	0.0178±0.0054	0.0125±0.0070	0.0081±0.0051
$A^{0,\mu}_{\rm FB}$	0.0182±0.0027	0.0172±0.0028	0.0168±0.0038	0.0137±0.0027
$A^{0,\tau}_{\rm FB}$	0.0202±0.0038	0.0200±0.0048	0.0287±0.0064	0.0183±0.0035
χ^2/d.o.f.	183/191	164/142	118/138	$10/6^{(a)}$

Table 3: Line shape and asymmetry parameters from 9-parameter fits to the data of the four LEP experiments.
$^{(a)}$This parameter set has been obtained from a parameter transformation applied to the 15 parameters of the OPAL fit [21], which treats the γZ interference terms for leptons as additional free parameters. The extra parameters for the γZ interference terms have been fixed to their Standard Model values in the transformation. The χ^2/d.o.f. for the 15-parameter fit to the data is 87/132.

Parameter	Average Value
$m_{\rm Z}$(GeV)	91.1884±0.0022
$\Gamma_{\rm Z}$(GeV)	2.4964±0.0032
$\sigma^0_{\rm h}$(nb)	41.490±0.078
$R_{\rm e}$	20.801±0.058
R_μ	20.795±0.043
R_τ	20.815±0.061
$A^{0,\rm e}_{\rm FB}$	0.0152±0.0027
$A^{0,\mu}_{\rm FB}$	0.0163±0.0015
$A^{0,\tau}_{\rm FB}$	0.0203±0.0022

Table 4: Average line shape and asymmetry parameters from the data of the four LEP experiments given in Table 3, without the assumption of lepton universality. The χ^2/d.o.f. of the average is 34/27.

	$m_{\rm Z}$	$\Gamma_{\rm Z}$	$\sigma^0_{\rm h}$	$R_{\rm e}$	R_μ	R_τ	$A^{0,\rm e}_{\rm FB}$	$A^{0,\mu}_{\rm FB}$	$A^{0,\tau}_{\rm FB}$
$m_{\rm Z}$	1.00	−0.08	0.02	0.03	−0.02	−0.01	0.02	0.07	0.04
$\Gamma_{\rm Z}$	−0.08	1.00	−0.12	−0.01	0.00	0.00	0.00	0.00	0.00
$\sigma^0_{\rm h}$	0.02	−0.12	1.00	0.08	0.12	0.08	0.01	0.00	0.00
$R_{\rm e}$	0.03	−0.01	0.08	1.00	0.08	0.03	−0.05	0.01	0.01
R_μ	−0.02	0.00	0.12	0.08	1.00	0.06	0.00	0.01	0.00
R_τ	−0.01	0.00	0.08	0.03	0.06	1.00	0.00	0.00	0.01
$A^{0,\rm e}_{\rm FB}$	0.02	0.00	0.01	−0.05	0.00	0.00	1.00	−0.04	−0.02
$A^{0,\mu}_{\rm FB}$	0.07	0.00	0.00	0.01	0.01	0.00	−0.04	1.00	0.07
$A^{0,\tau}_{\rm FB}$	0.04	0.00	0.00	0.01	0.00	0.01	−0.02	0.07	1.00

Table 5: The correlation matrix for the set of parameters given in Table 4.

	ALEPH	DELPHI	L3	OPAL
$m_{\rm Z}$(GeV)	91.1923±0.0037	91.1849±0.0034	91.1938±0.0036	91.1846±0.0035
$\Gamma_{\rm Z}$(GeV)	2.4952±0.0055	2.4917±0.0053	2.5022±0.0054	2.4959±0.0053
$\sigma^0_{\rm h}$(nb)	41.56±0.09	41.40±0.10	41.48±0.11	41.47±0.10
R_ℓ	20.738±0.060	20.704±0.073	20.811±0.076	20.851±0.059
$A^{0,\ell}_{\rm FB}$	0.0190±0.0020	0.0179±0.0023	0.0186±0.0030	0.0142±0.0020
χ^2/d.o.f.	189/195	165/146	122/142	15/10[(a)]

Table 6: Line shape and asymmetry parameters from 5-parameter fits to the data of the four LEP experiments, assuming lepton universality. R_ℓ is defined as $R_\ell \equiv \Gamma_{\rm had}/\Gamma_{\ell\ell}$, where $\Gamma_{\ell\ell}$ refers to the partial Z width for the decay into a pair of massless charged leptons.
[(a)]This parameter set has been obtained by a parameter transformation applied to the 15 parameters of the OPAL fit.

Parameter	Average Value
$m_{\rm Z}$(GeV)	91.1884±0.0022
$\Gamma_{\rm Z}$(GeV)	2.4964±0.0032
$\sigma^0_{\rm h}$(nb)	41.490±0.078
R_ℓ	20.789±0.032
$A^{0,\ell}_{\rm FB}$	0.0171±0.0011

Table 7: Average line shape and asymmetry parameters from the results of the four LEP experiments given in Table 6, assuming lepton universality. R_ℓ is defined as $R_\ell \equiv \Gamma_{\rm had}/\Gamma_{\ell\ell}$, where $\Gamma_{\ell\ell}$ refers to the partial Z width for the decay into a pair of massless charged leptons. The χ^2/d.o.f. of the average is 38/31.

	$m_{\rm Z}$	$\Gamma_{\rm Z}$	$\sigma^0_{\rm h}$	R_ℓ	$A^{0,\ell}_{\rm FB}$
$m_{\rm Z}$	1.00	−0.08	0.02	0.00	0.08
$\Gamma_{\rm Z}$	−0.08	1.00	−0.12	−0.01	0.00
$\sigma^0_{\rm h}$	0.02	−0.12	1.00	0.15	0.01
R_ℓ	0.00	−0.01	0.15	1.00	0.00
$A^{0,\ell}_{\rm FB}$	0.08	0.00	0.01	0.00	1.00

Table 8: The correlation matrix for the set of parameters given in Table 7.

Without Lepton Universality:		
$\Gamma_{\rm ee}$	(MeV)	83.91±0.17
$\Gamma_{\mu\mu}$	(MeV)	83.94±0.23
$\Gamma_{\tau\tau}$	(MeV)	83.86±0.31

With Lepton Universality:		
$\Gamma_{\ell\ell}$	(MeV)	83.94±0.14
$\Gamma_{\rm had}$	(MeV)	1745.0±3.0
$\Gamma_{\rm inv}$	(MeV)	499.7±2.5

Table 9: Partial decay widths of the Z boson, derived from the results of the 9-parameter (Tables 4 and 5) and the 5-parameter fit (Tables 7 and 8). In the case of lepton universality, $\Gamma_{\ell\ell}$ refers to the partial Z width for the decay into a pair of massless charged leptons.

3 The τ Polarization

The τ polarization, $\mathcal{P}_\tau$, is determined by an indirect measurement of the longitudinal polarization of τ pairs produced in Z decays. It is defined as:

$$\mathcal{P}_\tau \equiv \frac{\sigma_R - \sigma_L}{\sigma_R + \sigma_L}, \tag{4}$$

where σ_R and σ_L are the τ-pair cross sections for the production of a right-handed and left-handed τ^-, respectively. The angular distribution of $\mathcal{P}_\tau$ as a function of the angle θ between the e^- and the τ^-, for $\sqrt{s} = m_Z$, is given by:

$$\mathcal{P}_\tau(\cos\theta) = -\frac{\mathcal{A}_\tau(1+\cos^2\theta) + 2\mathcal{A}_e\cos\theta}{1+\cos^2\theta + 2\mathcal{A}_\tau\mathcal{A}_e\cos\theta}, \tag{5}$$

with $\mathcal{A}_e$ and $\mathcal{A}_\tau$ as defined in Equation (3). Equation (5) neglects corrections for the effects of γ exchange, γZ interference and electromagnetic radiative corrections for initial- and final-state radiation. These effects are, however, taken into account in the experimental analyses. In particular, these corrections account for the $\sqrt{s}$ dependence of the tau polarization, $\mathcal{P}_\tau(\cos\theta)$, which is important since the off-peak data are included in the event samples for all experiments. When averaged over all production angles $\mathcal{P}_\tau$ is a measurement of $\mathcal{A}_\tau$. As a function of $\cos\theta$, $\mathcal{P}_\tau(\cos\theta)$ provides nearly independent determinations of both $\mathcal{A}_\tau$ and $\mathcal{A}_e$, thus allowing a test of the universality of the couplings of the Z to e and τ.

Each experiment makes separate $\mathcal{P}_\tau$ measurements using the five τ decay modes $e\nu\overline{\nu}$, $\mu\nu\overline{\nu}$, $\pi\nu$, $\rho\nu$ and $a_1\nu$ [25–28]. The $\rho\nu$ and $\pi\nu$ are the most sensitive channels, contributing weights of about 40% each in the average. In addition, DELPHI has used an inclusive hadronic analysis. The combination is made of the results from each experiment already averaged over the τ decay modes.

A discussion of the effects of possible common systematic errors between the experiments can be found in [3]. Further study of the uncertainties from the effects of radiative corrections for the ρ decay mode of the τ is desirable.

3.1 Results

Tables 10 and 11 show the most recent results for $\mathcal{A}_\tau$ and $\mathcal{A}_e$ obtained by the four experiments [25–28] and their combination. No common systematics are included in these averages. The statistical correlation between the extracted values of $\mathcal{A}_\tau$ and $\mathcal{A}_e$ is small ($\leq 5\%$), and is neglected.

The average values for $\mathcal{A}_\tau$ and $\mathcal{A}_e$:

$$\mathcal{A}_\tau = 0.1394 \pm 0.0069 \tag{6}$$
$$\mathcal{A}_e = 0.1429 \pm 0.0079, \tag{7}$$

are compatible, as is expected from lepton universality. Assuming $e - \tau$ universality, the values for $\mathcal{A}_\tau$ and $\mathcal{A}_e$ can be combined. This combination is performed neglecting any possible common systematic error between $\mathcal{A}_\tau$ and $\mathcal{A}_e$ within a given experiment. Such errors are estimated to be small, but warrant further study. The combined result of $\mathcal{A}_\tau$ and $\mathcal{A}_e$ gives:

$$\mathcal{A}_\ell = 0.1409 \pm 0.0052. \tag{8}$$

ALEPH	('90 - '92), final	$0.136 \pm 0.012 \pm 0.009$
DELPHI	('90 - '94), prel.	$0.135 \pm 0.009 \pm 0.010$
L3	('90 - '94), prel.	$0.152 \pm 0.010 \pm 0.009$
OPAL	('90 - '94), prel.	$0.134 \pm 0.010 \pm 0.009$
LEP Average		0.1394 ± 0.0069

Table 10: LEP results for $\mathcal{A}_\tau$. The χ^2/d.o.f. for the average is 1.2/3. The first error is statistical and the second systematic. In the LEP average, statistical and systematic error are combined in quadrature. The systematic component of the error, obtained by combining the individual systematic errors, is ± 0.0046.

ALEPH	('90 - '92), final	$0.129 \pm 0.016 \pm 0.005$
DELPHI	('90 - '94), prel.	$0.151 \pm 0.014 \pm 0.003$
L3	('90 - '94), prel.	$0.156 \pm 0.016 \pm 0.005$
OPAL	('90 - '94), prel.	$0.134 \pm 0.015 \pm 0.004$
LEP Average		0.1429 ± 0.0079

Table 11: LEP results for $\mathcal{A}_e$. The χ^2/d.o.f. for the average is 2.0/3. The first error is statistical and the second systematic. In the LEP average, statistical and systematic error are combined in quadrature. The systematic component of the error, obtained by combining the individual systematic errors, is ± 0.0020.

4 Results from b and c Quarks

The relevant quantities measured in the heavy quark sector at LEP are:

- The ratios of the b and c quark partial widths of the Z to its total hadronic partial width: $R_{\mathrm{b}} \equiv \Gamma_{\mathrm{b\bar{b}}}/\Gamma_{\mathrm{had}}$ and $R_{\mathrm{c}} \equiv \Gamma_{\mathrm{c\bar{c}}}/\Gamma_{\mathrm{had}}$.
- The forward-backward asymmetries, $A_{\mathrm{FB}}^{\mathrm{b\bar{b}}}$ and $A_{\mathrm{FB}}^{\mathrm{c\bar{c}}}$.
- The semileptonic branching ratios, $\mathrm{BR}(\mathrm{b} \to \ell)$ and $\mathrm{BR}(\mathrm{b} \to \mathrm{c} \to \bar{\ell})$, and the average $\mathrm{B}^0\overline{\mathrm{B}^0}$ mixing parameter, $\overline{\chi}$. These are often determined at the same time as the widths or asymmetries in multi-parameter fits to lepton tag samples. They are included in the combination procedure to take into account their correlations with the other parameters measured in the same fit.
- The probability that a c-quark fragments into a D^{*+} times the branching ratio of the D^{*+} to decay into $\pi^+\mathrm{D}^0$, $\mathrm{P}(\mathrm{c} \to \mathrm{D}^{*+}) \times \mathrm{BR}(\mathrm{D}^{*+} \to \pi^+\mathrm{D}^0)$. This quantity is determined now with good accuracy by the LEP experiments, so that the interpretation of the D^* rate in terms of R_c can be done without assumptions on the energy dependence of the D-meson production rate.

There are several motivations for the averaging procedure. Several analyses measure more than one parameter simultaneously, for example the lepton fits. Some of the measurements of electroweak parameters depend explicitly on the values of other parameters, for example R_{b} depends on R_{c}. The common tagging and analysis techniques lead to common sources of systematic uncertainty, in particular for the double-tag measurements of R_{b}. The starting point for the combination is to ensure that all the analyses use a common set of assumptions for input parameters which give rise to systematic uncertainties [4]. The correlations and interdependences of the input measurements are then taken into account in a χ^2 minimization which results in the combined electroweak parameters and their correlation matrix. The only significant correlation between any of the resulting electroweak parameters turns out to be between R_{b} and R_{c}. This is discussed at the end of this section.

In a first fit the asymmetry measurements on peak, above peak and below peak were combined at each centre-of-mass energy. The results of this fit, including the SLD results, are given in the appendix. The dependence of the average asymmetries on centre-of-mass energy agrees with the prediction of the Standard Model. To derive the pole asymmetries, $A_{\mathrm{FB}}^{0,\mathrm{q}}$, from the quark asymmetries, all the off-peak asymmetry measurements were then corrected to the peak energy before combining. Only results from this second fit are quoted here. There are therefore 8 parameters in total to be determined in the combination procedure: the two partial widths, two asymmetries, two semileptonic branching ratios, the average mixing parameter and the probability for c quark to fragment into a D^{*+}.

Recently the SLD collaboration has presented precise measurements of R_{b} [8] and of the left-right forward-backward asymmetry for b and c quarks [7]. Since the precision and the dominant sources of systematic uncertainty are similar at LEP and SLD it is useful to produce combined LEP+SLD averages. The left-right forward-backward asymmetries are, in contrast to the unpolarized forward-backward asymmetries, only sensitive to the final state couplings ($\mathcal{A}_{\mathrm{b}}$ and $\mathcal{A}_{\mathrm{c}}$). They are treated in the averaging procedure as physically independent quantities. However the methods to measure the polarized and unpolarized asymmetries are very similar, so $\mathcal{A}_{\mathrm{b}}$ and $\mathcal{A}_{\mathrm{c}}$ are included in the averaging procedure in order to estimate the correlation between the SLD and the LEP asymmetries, resulting in a 10-parameter fit.

4.1 Summary of measurements and averaging procedure

The measurements of $R_{\rm b}$ and $R_{\rm c}$ fall into two categories. In the first, called a single-tag measurement, a method to select b or c events is devised, and the number of tagged events is counted. This number must then be corrected for backgrounds from other flavours and for the tagging efficiency to calculate the true fraction of hadronic Z decays of that flavour. The dominant systematic errors come from understanding the branching ratios and detection efficiencies which give the overall tagging efficiency. For the second technique, called a double-tag measurement, the event is divided into two hemispheres. For an $R_{\rm b}$ measurement, writing the number of tagged single hemispheres as N_t, the number of events with both hemispheres tagged as N_{tt}, then for a total of $N_{\rm had}$ hadronic Z decays:

$$\begin{aligned} \frac{N_t}{2N_{\rm had}} &= \varepsilon_{\rm b}R_{\rm b} + \varepsilon_{\rm c}R_{\rm c} + \varepsilon_{\rm uds}(1 - R_{\rm b} - R_{\rm c}), \\ \frac{N_{tt}}{N_{\rm had}} &= \mathcal{C}_{\rm b}\varepsilon_{\rm b}^2 R_{\rm b} + \varepsilon_{\rm c}^2 R_{\rm c} + \varepsilon_{\rm uds}^2(1 - R_{\rm b} - R_{\rm c}), \end{aligned}$$

where $\varepsilon_{\rm b}$, $\varepsilon_{\rm c}$ and $\varepsilon_{\rm uds}$ are the tagging efficiencies per hemisphere for b, c and light-quark events, and $\mathcal{C}_{\rm b} \neq 1$ accounts for the fact that the tagging efficiencies between the hemispheres may be correlated. In practice, $\varepsilon_{\rm b} \gg \varepsilon_{\rm c} \gg \varepsilon_{\rm uds}$, $\mathcal{C}_{\rm b} \approx 1$, and the correlations for the other flavours are neglected. These equations can be solved to give $R_{\rm b}$ and $\varepsilon_{\rm b}$, which neglecting the c and uds backgrounds and the correlations are approximately given by:

$$\begin{aligned} \varepsilon_{\rm b} &\approx 2N_{tt}/N_t, \\ R_{\rm b} &\approx N_t^2/(4N_{tt}N_{\rm had}). \end{aligned}$$

The double-tagging method has the advantage that the tagging efficiency is derived directly from the data, reducing the systematic error of the measurement. The residual background of other flavours in the sample, and the evaluation of the correlation between the tagging efficiencies in the two hemispheres of the event are the main sources of systematic uncertainty in such an analysis.

The measurements included are:

- Lepton fits from all four LEP experiments [29–33]. Each fit measures several parameters chosen from: $R_{\rm b}$, $R_{\rm c}$, $A_{\rm FB}^{\rm b\bar{b}}$, $A_{\rm FB}^{\rm c\bar{c}}$, BR(b $\to \ell$) and BR(b $\to$ c $\to \bar{\ell}$), and $\overline{\chi}$. The measured parameters are correlated. These analyses use hadronic events with one or more leptons in the final state. The semileptonic branching ratios can therefore be measured by a double-tagging technique if the lepton identification efficiency is known. The dominant sources of systematic error for the lepton fits arise from the lepton identification, from other semileptonic branching ratios and from the modeling of the semileptonic decay.

- Event-shape tag for $R_{\rm b}$ from ALEPH (double tag) and L3 (single tag) [34,35].

- Lifetime (and lepton) double tag measurements for $R_{\rm b}$ from ALEPH, DELPHI, OPAL and SLD [8,36–38]. These are the most precise determinations of $R_{\rm b}$, and dominate the combined result. The features of the double-tag technique were discussed above. These results depend explicitly on the assumed value of $R_{\rm c}$.

- Measurements of $A_{\rm FB}^{\rm b\bar{b}}$ based on lifetime tagged events with a hemisphere charge measurement from ALEPH , DELPHI and OPAL where the mean b-hemisphere charge is derived from the charge distributions themselves [31,39,40]. These contribute roughly the same weight to the combined result as the lepton fits.

- Analyses with $D/D^{*\pm}$ mesons to measure R_c from DELPHI and OPAL [41, 42]. For the first time all measurements are constructed in a way that in principle no assumptions on the energy dependence of charm fragmentation are necessary. However in practice the low energy contraint still improves the obtainable precision by about 10% and is thus included in the average. The available measurements can be divided into three groups:
  - inclusive/exclusive double tag (DELPHI, OPAL): In a first step $D^{*\pm}$ mesons are reconstructed in several decay channels and their production rate is measured, which depends on the product $R_c \times P(c \to D^{*+}) \times BR(D^{*+} \to \pi^+ D^0)$. This sample of clean $c\overline{c}$ (and $b\overline{b}$) events is then used to measure $P(c \to D^{*+}) \times BR(D^{*+} \to \pi^+ D^0)$ using a slow pion tag in the opposite hemisphere.
  - inclusive single/double tag (DELPHI): This measurement measures the single and double tag rate using a slow pion tag. It takes advantage of the much higher efficiency of the inclusive slow pion tag compared to the exclusive reconstruction, however it suffers from problems due to the high background.
  - Reconstruction of all weakly decaying D states (DELPHI, OPAL): These analyses make the assumption that the production rates of D^0, D^+, D_s and Λ_c saturate the fragmentation of $c\overline{c}$, since every charm quark ends up in a ground state hadron before the weak decay. This is a single tag measurement, but is insensitive to uncertainties in the charm hadronisation, relying only on the decay branching ratios of the charm hadrons.
- Analyses with a $D^{*\pm}$ meson to measure $A_{FB}^{c\bar{c}}$ and $A_{FB}^{b\bar{b}}$ from ALEPH, DELPHI and OPAL [31, 43, 44].
- Measurements of $\mathcal{A}_b$ and $\mathcal{A}_c$ from SLD [7]. These results use lepton, kaon, $D^{*\pm}$ and lifetime plus hemisphere charge tags, with similar sources of systematic error as the LEP asymmetry measurements.

These measurements are presented by the LEP and SLD collaborations in a consistent manner for the purpose of combination [4]. The tables prepared by the experiments include a detailed breakdown of the systematic error of each measurement and its dependence on other electroweak parameters. Where necessary, the experiments apply small corrections to their results in order to use agreed values and ranges for the input parameters used to calculate systematic errors. The measurements, corrected where necessary, are summarized in the Appendix in Tables 25-34, where the statistical and systematic errors are quoted separately. The correlated systematic entries are from sources shared with one or more other results in the table and are derived from the full breakdown of common systematic uncertainties. The uncorrelated systematic entries are from the remaining sources.

The χ^2 minimization procedure used to derive the values of the heavy-flavour electroweak parameters was published in [4]. The explicit dependences of each measurement on the other parameters is taken into account, for example the dependence of the value of R_b on the assumed value of R_c as described below. The full statistical and systematic covariance matrix for all the measurements is calculated. The correlation matrices relating several measurements made in the same analyses are used, in particular for the multi-parameter lepton fits. Additional correlations arising from common sources of systematic uncertainty are estimated from a detailed breakdown of systematic errors. For the common systematic errors, this breakdown for the double-tag measurements of R_b, plus the L3 event-shape analysis which also measures this single parameter, is given for illustration in Table 12. Similarly, a list of the correlated systematic errors for measurements of R_c relying on D and $D^{*\pm}$ mesons is given in Table 13.

Since c-quark events form the main background in the R_b analyses, the value of R_b depends on the value of R_c. If R_b and R_c are measured in the same analysis, this is reflected in the correlation

matrix for the results. Otherwise the normalization of the charm contribution is not fixed by the data, and the measurement of $R_{\rm b}$ depends on the assumed value of $R_{\rm c}$, which may be written as:

$$R_{\rm b} = R_{\rm b}^{\rm meas} + a(R_{\rm c})\frac{(R_{\rm c} - R_{\rm c}^{\rm used})}{R_{\rm c}}. \tag{9}$$

In this expression, $R_{\rm b}^{\rm meas}$ is the result of the analysis assuming a value of $R_{\rm c} = R_{\rm c}^{\rm used}$. The values

	ALEPH shape [34]	ALEPH lifetime [36]	DELPHI multiple [37]	L3 shape [35]	OPAL multiple [38]	SLD lifetime [8]
Charm production	0.0	−0.85	−1.2	0.0	−0.94	−0.57
D^0 lifetime	0.0	−0.28	−0.2	0.0	−0.23	−0.08
D^+ lifetime	0.0	−0.36	−0.2	0.0	−0.29	−0.01
D_s lifetime	0.0	−0.22	−0.2	0.0	−0.17	−0.05
D decay multiplicity	0.0	−0.57	−0.4	0.0	−0.76	−0.20
BR(D→K^0)	0.0	0.0	+0.6	0.0	+0.59	0.37
Gluon splitting: g → $b\bar{b}, c\bar{c}$	0.0	−0.33	−0.2	0.0	−0.46	−0.41
Long-lived light hadrons	0.0	−0.24	−0.4	0.0	−0.33	−0.10
BR(c → ℓ)	+0.6	0.0	−0.2	0.0	−0.28	0.0
Semileptonic model c → ℓ	−2.1	0.0	−0.2	0.0	−0.25	0.0
$\langle x_E(c)\rangle$	+0.8	−0.12	−0.4	+1.8	−0.75	−0.26
Semileptonic model b → ℓ	−1.3	0.0	+0.2	0.0	0.0	0.0
$\langle x_E(b)\rangle$	0.0	0.0	0.0	−3.1	0.0	0.0
Total	2.7	1.2	1.6	3.6	1.7	0.9

Table 12: Example of breakdown of the correlated systematic error for $R_{\rm b}$ from lifetime, multiple and shape double-tag measurements (in units of 10^{-3}). The sign indicates the correlation of the measurement with the parameter describing the source of the error.

	DELPHI $D^{*\pm}$ incl./excl. [41]	DELPHI D^0, D^+, D_s, Λ_c [41]	OPAL $D^{*\pm}$ [42]	OPAL D^0, D^+, D_s, Λ_c [42]
$\langle x_E(c)\rangle$	0.000	0.005	0.006	0.007
$\langle x_E(b)\rangle$	0.000	0.007	0.000	0.003
Gluon splitting: g → $c\bar{c}$	0.000	0.001	0.003	0.002
BR(c → D^* → $K\pi\pi_s$)	0.005	0.000	0.007	0.000
B lifetime	0.000	0.004	0.002	0.005
D decay multiplicity and lifetime	0.000	0.001	0.001	0.006
D decay branching ratios	0.001	0.005	0.004	0.005
Total	0.005	0.010	0.011	0.012

Table 13: Breakdown of the correlated systematic errors for $R_{\rm c}$ from D and $D^{*\pm}$ related measurements. The inclusive DELPHI measurements is a double-tag method. The OPAL measurement denoted as $D^{*\pm}$ is a combination of the single tag $D^{*\pm}$ based analysis, and the measurement of BR(c → D^* → $K\pi\pi_s$) using a double tag.

of $R_{\rm c}^{\rm used}$ and the coefficients $a(R_{\rm c})$ are given in Table 25 where appropriate. The dependences of all other measurements on other electroweak parameters are treated in the same way, with coefficients $a(x)$ describing the dependence on parameter x.

4.2 Treatment of the LEP Asymmetry Measurements

For the 8-parameter fit described above, the peak and off-peak asymmetries were corrected to $\sqrt{s} = 91.26\,\mathrm{GeV}$, using the predicted dependence from ZFITTER [45]. The slope of the asymmetry around m_Z depends only on the axial coupling and the charge of the initial and final state fermions and is thus independent of the value of the asymmetry itself.

After calculating the overall averages, the quark pole asymmetries, $A_{FB}^{0,q}$, were derived by applying the corrections described below. The input measured asymmetries are all corrected to full acceptance and use the thrust axis as an estimate of the quark direction before gluon radiation. To relate the pole asymmetries to these numbers a few corrections that are summarized in Table 14 have to be applied:

- Energy shift to $\sqrt{s} = m_Z$ and QED corrections: The corrections due to the energy shift and initial state radiation have been calculated using ZFITTER [45].
- QCD corrections: The QCD corrections, using the thrust axis to define θ for the event, have been calculated to first order, including mass corrections [46]. The correction is given by $A_{FB}^{QCD} = A_{FB}^{no\,QCD}(1 + c\frac{\alpha_s}{\pi})$, with $c = -0.87$ for charm and $c = -0.79$ for bottom quarks. Assuming $\alpha_s(m_Z^2) = 0.12$ and varying the renormalization scale between $\mu^2 = (m_Z/4)^2$ and $\mu^2 = m_Z^2$ the correction factor is 0.966 ± 0.004 for b quarks, and 0.963 ± 0.004 for c quarks. There is an additional uncertainty in the QCD correction coming from whether the experimental event selection requirements bias the relative rates of 2- and 3-jet events in the sample. The error on the correction factor has therefore been increased to 0.010 for both b and c quarks. The resulting additive corrections to the asymmetries due to QCD corrections are provided in Table 14.
- γ exchange, γZ interference: These very small corrections have again been calculated using ZFITTER.

The lifetime/jet-charge measurements of asymmetries take into account QCD effects as an inherent part of the analysis, but the measured asymmetries for the analyses using a lepton or D^* tag need to be corrected for the effects of QCD on the event thrust axis direction. In order to perform a consistent average with the other asymmetry measurements, the jet-charge measurements were adjusted by subtracting 0.0033 from each of the three $A_{FB}^{b\bar{b}}(\mathrm{pk})$ jet-charge measurements before averaging.

Source	δA_{FB}^{b}	δA_{FB}^{c}
$\sqrt{s} = m_Z$	−0.0013	−0.0034
QED corrections	+0.0041	+0.0104
QCD corrections	$+0.0033 \pm 0.0010$	$+0.0023 \pm 0.0007$
γ, γZ	−0.0003	−0.0008
Total	$+0.0058 \pm 0.0010$	$+0.0085 \pm 0.0007$

Table 14: Corrections to be applied to the quark asymmetries. The corrections are to be understood as $A_{FB}^{0} = A_{FB}^{meas} + \sum_i (\delta A_{FB})_i$

4.3 Results

4.3.1 Results of the 8-parameter fit to LEP data

Using the full averaging procedure gives the following combined results for the electroweak parameters:

$$
\begin{aligned}
R_{\mathrm{b}}^{0} &= 0.2215 \pm 0.0017 \\
R_{\mathrm{c}}^{0} &= 0.1596 \pm 0.0070 \\
A_{\mathrm{FB}}^{0,\mathrm{b}} &= 0.1002 \pm 0.0028 \\
A_{\mathrm{FB}}^{0,\mathrm{c}} &= 0.0756 \pm 0.0051\,,
\end{aligned}
\tag{10}
$$

where all corrections to the asymmetries and partial widths have been already applied. The χ^2/dof is $40/(70-8)$. The corresponding correlation matrix is given in Table 15. For these results an external constraint of $\mathrm{P}(\mathrm{c} \to \mathrm{D}^{*+}) \times \mathrm{BR}(\mathrm{D}^{*+} \to \pi^{+}\mathrm{D}^{0}) = 0.179 \pm 0.013$ from low energy measurements has been applied. If this constraint is dropped R_{c}^{0} moves to $R_{\mathrm{c}}^{0} = 0.1626 \pm 0.0076$. The product $\mathrm{P}(\mathrm{c} \to \mathrm{D}^{*+}) \times \mathrm{BR}(\mathrm{D}^{*+} \to \pi^{+}\mathrm{D}^{0})$ is measured by the LEP experiments to be 0.1644 ± 0.0080, very consistent with the low energy data. If R_{c}^{0} is fixed to its Standard-Model prediction of 0.172, then the value of R_{b}^{0} is:

$$
R_{\mathrm{b}}^{0}(R_{\mathrm{c}}^{0} = 0.172) \;=\; 0.2206 \pm 0.0016\,.
$$

	R_{b}^{0}	R_{c}^{0}	$A_{\mathrm{FB}}^{0,\mathrm{b}}$	$A_{\mathrm{FB}}^{0,\mathrm{c}}$
R_{b}^{0}	1.00	–0.30	0.00	–0.02
R_{c}^{0}	–0.30	1.00	0.05	0.01
$A_{\mathrm{FB}}^{0,\mathrm{b}}$	0.00	0.05	1.00	0.09
$A_{\mathrm{FB}}^{0,\mathrm{c}}$	–0.02	0.01	0.09	1.00

Table 15: The correlation matrix for the electroweak parameters from the 8-parameter fit

4.3.2 Results of the 10-parameter fit to LEP and SLD data

Including the SLD results on R_b, $\mathcal{A}_b$ and $\mathcal{A}_c$ into the fit the following results are obtained:

$$\begin{aligned} R_b^0 &= 0.2211 \pm 0.0016 \\ R_c^0 &= 0.1598 \pm 0.0069 \\ A_{FB}^{0,b} &= 0.1002 \pm 0.0028 \\ A_{FB}^{0,c} &= 0.0759 \pm 0.0051 \\ \mathcal{A}_b &= 0.842 \pm 0.052 \\ \mathcal{A}_c &= 0.618 \pm 0.091\,, \end{aligned} \tag{11}$$

with a χ^2/dof of $41/(76-10)$. The corresponding correlation matrix is given in Table 16. In deriving these results the parameters $\mathcal{A}_b$ and $\mathcal{A}_c$ have been treated as independent of the forward-backward asymmetries $A_{FB}^{b\bar{b}}(\mathrm{pk})$ and $A_{FB}^{c\bar{c}}(\mathrm{pk})$. The fit results of $\mathcal{A}_b$ and $\mathcal{A}_c$ take into account the LEP and SLD average values of R_b and R_c, whereas the input numbers assumed the Standard Model values. This accounts for the fit results being lower than the input measurements.

	R_b^0	R_c^0	$A_{FB}^{0,b}$	$A_{FB}^{0,c}$	$\mathcal{A}_b$	$\mathcal{A}_c$
R_b^0	1.00	–0.30	0.01	–0.03	–0.06	0.05
R_c^0	–0.30	1.00	0.05	0.02	0.07	–0.06
$A_{FB}^{0,b}$	0.01	0.05	1.00	0.10	0.04	0.00
$A_{FB}^{0,b}$	–0.03	0.02	0.10	1.00	–0.01	0.06
$\mathcal{A}_b$	–0.06	0.07	0.04	–0.01	1.00	0.07
$\mathcal{A}_c$	0.05	–0.06	0.00	0.06	0.07	1.00

Table 16: The correlation matrix for the electroweak parameters from the 10-parameter fit

If R_c^0 is fixed to its Standard-Model prediction of 0.172, then the value of R_b^0 is:

$$R_b^0(R_c^0 = 0.172) = 0.2202 \pm 0.0016\,.$$

It is not yet clear to what extent the uncertainty in the QCD correction is correlated between the LEP and SLD results. The possible correlation has been neglected here. If one assumes this error to be fully correlated the correlation between $A_{FB}^{0,b}$ and $\mathcal{A}_b$ would increase by 0.05. All other elements of the correlation matrix remain unchanged.

The result of the full fit to the LEP/SLC results including the off peak asymmetries can be found in the appendix.

4.4 Comments on the correlation between R_b and R_c

As noted before, the only large correlation between any of the combined electroweak parameters in Equations 10 and 11 is between R_b and R_c. It is useful to examine how the correlations and interdependencies of the input measurements lead to this correlation between the combined parameters.

The measurements of R_c are almost independent of an assumed value for R_b. For the lepton fit analyses, there is a very small net correlation between the two partial widths. There is a negative

statistical correlation from events moving between the b and c contributions to the lepton sample. The overall systematic correlation is positive, dominated by effects such as the subtraction of hadronic background to the lepton sample, or the lepton identification efficiency which affect the b and c contributions in the same way. The net correlation from statistical and systematic effects is small.

The D and D^* meson measurements of R_c are constructed to be independent of an assumed value for R_b, because they make a statistical separation of the b and c contributions based on other event properties. The overall normalization of the b contribution is therefore fixed by the data. These results depend on the features of b-hadron decay, but not on an assumed value of R_b.

The precise double-tag measurements of R_b dominate the combined R_b result. The value of R_b from these measurements depend explicitly on the value of R_c assumed, and this dependence combined with the current error on R_c is almost entirely responsible for the size of the correlation coefficient between R_b and R_c.

5 The Hadronic Charge Asymmetry $\langle Q_{FB} \rangle$

The LEP experiments ALEPH [47–49], DELPHI [50, 51], and OPAL [52, 53] have provided measurements of the hadronic charge asymmetry based on the mean difference in jet charges measured in the forward and backward event hemispheres, $\langle Q_{FB} \rangle$. DELPHI has also provided a related measurement of the total charge asymmetry by making a charge assignment on an event-by-event basis and performing a likelihood fit [50]. The experimental values quoted for the average forward-backward charge difference $\langle Q_{FB} \rangle$, cannot be directly compared as some of them include detector dependent effects such as acceptances and efficiencies. We therefore use the effective electroweak mixing angle, $\sin^2\theta^{lept}_{eff}$, defined in Section 6.3, as a means of combining the experimental results summarized in Table 17.

Experiment		$\sin^2\theta^{lept}_{eff}$
ALEPH	90-94, final	$0.2322 \pm 0.0008 \pm 0.0011$
DELPHI	91-94, prel.	$0.2311 \pm 0.0010 \pm 0.0014$
OPAL	91-94, prel.	$0.2326 \pm 0.0012 \pm 0.0013$
Average		0.2320 ± 0.0010

Table 17: Summary of the determination of $\sin^2\theta^{lept}_{eff}$ from inclusive hadronic charge asymmetries at LEP. For each experiment, the first error is statistical and the second systematic. The latter is dominated by fragmentation and decay modeling uncertainties.

The dominant source of systematic error arises from the modeling of the charge flow in the fragmentation process for each flavour. All experiments measure the required charge properties for $Z \to b\bar{b}$ events from the data. ALEPH also determine the charm charge properties from the data. The fragmentation model implemented in the JETSET Monte-Carlo program [54] is used by all experiments as reference; the one of the HERWIG Monte-Carlo program [55] is used for comparison. The JETSET fragmentation parameters are varied to estimate the systematic errors. The central values chosen by the experiments for these parameters are, however, not the same. The degree of correlation between the fragmentation uncertainties for the different experiments requires further investigation. We treat the smaller of the two fragmentation errors in any pair of results as common to both. The present average of $\sin^2\theta^{lept}_{eff}$ from $\langle Q_{FB} \rangle$ and its associated error are not very sensitive to the treatment of common uncertainties.

The ambiguities due to QCD corrections may cause changes in the derived value of $\sin^2\theta^{lept}_{eff}$. These are, however, well below the fragmentation uncertainties and experimental errors. The effect of fully correlating the estimated systematic uncertainties from this source between the experiments on the average and its error is negligible.

There is also some correlation between these results and those for $A^{b\bar{b}}_{FB}$ using jet charges. The dominant source of correlation is again through uncertainties in the fragmentation and decay models used. The typical correlation between the derived values of $\sin^2\theta^{lept}_{eff}$ between the $\langle Q_{FB} \rangle$ and the $A^{b\bar{b}}_{FB}$ jet charge measurement has been estimated to be between 20% and 25%. This leads to only a small change in the relative weights for the $A^{b\bar{b}}_{FB}$ and $\langle Q_{FB} \rangle$ results when averaging their $\sin^2\theta^{lept}_{eff}$ values (Section 6.3). Furthermore, the jet charge method contributes at most half of the weight of the $A^{b\bar{b}}_{FB}$ measurement. Thus, the correlation between $\langle Q_{FB} \rangle$ and $A^{b\bar{b}}_{FB}$ from jet charge will have little impact on the overall Standard Model fit, and is neglected at present.

6 Interpretation of Results

6.1 The Coupling Parameters $\mathcal{A}_f$

The coupling parameters $\mathcal{A}_f$ are defined in terms of the effective vector and axial-vector neutral current couplings of fermions (Equation (3)). The LEP measurements of the forward-backward asymmetries of charged leptons (Section 2) and b and c quarks (Section 4) determine the products $A_{FB}^{0,f} = \frac{3}{4}\mathcal{A}_e\mathcal{A}_f$ (Equation (2)). The LEP measurements of the τ polarization (Section 3), $\mathcal{P}_\tau(\cos\theta)$, determine $\mathcal{A}_\tau$ and $\mathcal{A}_e$ separately (Equation (5)). The SLD collaboration measures the left-right asymmetry, A_{LR} [5, 6], which determines the same quantity, $\mathcal{A}_e$, as the τ polarization, with minimal model dependence. Both measurements have small systematic errors. The SLD measurements of the left-right forward-backward asymmetries for b and c quarks [7] are direct determinations of $\mathcal{A}_b$ and $\mathcal{A}_c$.

Table 18 shows the results on the leptonic coupling parameter $\mathcal{A}_\ell$ and their combination assuming lepton universality. Table 19 shows the results on the quark coupling parameters $\mathcal{A}_b$ and $\mathcal{A}_c$ derived from LEP measurements alone (Equation 10) and from the combination of LEP and SLD measurements (Equation 11).

	$\mathcal{A}_\ell$	Cumulative Average	χ^2/d.o.f.
$A_{FB}^{0,\ell}$	0.1510 ± 0.0049		
$\mathcal{P}_\tau(\cos\theta)$	0.1409 ± 0.0052	0.1463 ± 0.0036	2.0/1
A_{LR} (SLD)	0.1551 ± 0.0040	0.1502 ± 0.0027	4.7/2

Table 18: Comparison of the determinations of the leptonic coupling parameter $\mathcal{A}_\ell$ assuming lepton universality. The second column lists the $\mathcal{A}_\ell$ values derived from the quantities listed in the first column. The third column contains the cumulative averages of these $\mathcal{A}_\ell$ results. The averages are derived assuming no correlations between the measurements. The χ^2 per degree of freedom for the cumulative averages is given in the last column.

LEP	using $\mathcal{A}_\ell = 0.1463 \pm 0.0036$
$\mathcal{A}_b$	0.913 ± 0.034
$\mathcal{A}_c$	0.689 ± 0.050
LEP+SLD	**using $\mathcal{A}_\ell = 0.1502 \pm 0.0027$**
$\mathcal{A}_b$	0.878 ± 0.026
$\mathcal{A}_c$	0.662 ± 0.042

Table 19: Determinations of the quark coupling parameters $\mathcal{A}_b$ and $\mathcal{A}_c$ from LEP data alone (using the LEP average for $\mathcal{A}_\ell$) and from LEP+SLD data (using the LEP+SLD average for $\mathcal{A}_\ell$) assuming lepton universality.

6.2 The Effective Vector and Axial-Vector Coupling Constants

The partial widths of the Z into leptons and the lepton forward-backward asymmetries (Section 2), the τ polarization and the τ polarization asymmetry (Section 3) can be combined to determine the effective vector and axial-vector couplings for e, μ and τ. The asymmetries (Equations (2) and (5)) determine the ratio $g_{V\ell}/g_{A\ell}$ (Equation (3)), while the sum of the squares of the couplings is derived from the leptonic partial widths:

$$\Gamma_{\ell\ell} = \frac{G_{\rm F} m_{\rm Z}^3}{6\pi\sqrt{2}}(g_{V\ell}^2 + g_{A\ell}^2)(1+\delta_\ell^{QED}), \tag{12}$$

where $\delta_\ell^{QED} = 3q_\ell^2\alpha(m_{\rm Z}^2)/(4\pi)$ accounts for final state photonic corrections. Corrections due to lepton masses, neglected in Equation 12, are taken into account for the results presented below.

The averaged results for the effective lepton couplings are given in Table 20. Figure 2 shows the 68% probability contours in the $g_{A\ell}$-$g_{V\ell}$ plane. The signs of $g_{A\ell}$ and $g_{V\ell}$ are based on the convention $g_{A{\rm e}} < 0$. With this convention the signs of the couplings of all charged leptons follow from LEP data alone. For comparison, the $g_{V\ell}$-$g_{A\ell}$ relation following from the measurement of $A_{\rm LR}$ from SLD [5,6] is indicated as a band in the $g_{A\ell}$-$g_{V\ell}$-plane of Figure 2. It is consistent with the LEP data. The information on the leptonic couplings from LEP can therefore be combined with the $A_{\rm LR}$ measurement of SLD. The results for this combination are given in the right column of Table 20. The measured ratios of the e, μ and τ couplings provide a test of lepton universality and are also given in Table 20.

	Without Lepton Universality:	
	LEP	LEP+SLD
$g_{V{\rm e}}$	-0.0371 ± 0.0016	-0.03853 ± 0.00084
$g_{V\mu}$	-0.0367 ± 0.0038	-0.0353 ± 0.0034
$g_{V\tau}$	-0.0363 ± 0.0017	-0.0362 ± 0.0016
$g_{A{\rm e}}$	-0.50112 ± 0.00051	-0.50102 ± 0.00051
$g_{A\mu}$	-0.50120 ± 0.00075	-0.50129 ± 0.00074
$g_{A\tau}$	-0.50157 ± 0.00089	-0.50157 ± 0.00089
	Ratios of couplings:	
	LEP	LEP+SLD
$g_{V\mu}/g_{V{\rm e}}$	0.99 ± 0.13	0.916 ± 0.095
$g_{V\tau}/g_{V{\rm e}}$	0.980 ± 0.064	0.940 ± 0.048
$g_{A\mu}/g_{A{\rm e}}$	1.0000 ± 0.0018	1.0005 ± 0.0017
$g_{A\tau}/g_{A{\rm e}}$	1.0009 ± 0.0020	1.0011 ± 0.0020
	With Lepton Universality:	
	LEP	LEP+SLD
$g_{V\ell}$	-0.03677 ± 0.00094	-0.03785 ± 0.00068
$g_{A\ell}$	-0.50120 ± 0.00041	-0.50112 ± 0.00041
g_ν	$+0.5011 \pm 0.0013$	$+0.5011 \pm 0.0013$

Table 20: Results for the effective vector and axial-vector couplings derived from the combined LEP data without and with the assumption of lepton universality. For the right column the SLD measurement of $A_{\rm LR}$ is also included.

The neutrino couplings to the Z can be derived from the measured value of its invisible width, $\Gamma_{\rm inv}$, attributing it exclusively to the decay into three identical neutrino generations ($\Gamma_{\rm inv} = 3\Gamma_{\nu\nu}$) and assuming $g_{A\nu} \equiv g_{V\nu} \equiv g_\nu$. The relative sign of g_ν is chosen to be in agreement with neutrino scattering data [56], resulting in $g_\nu = +0.5011 \pm 0.0013$.

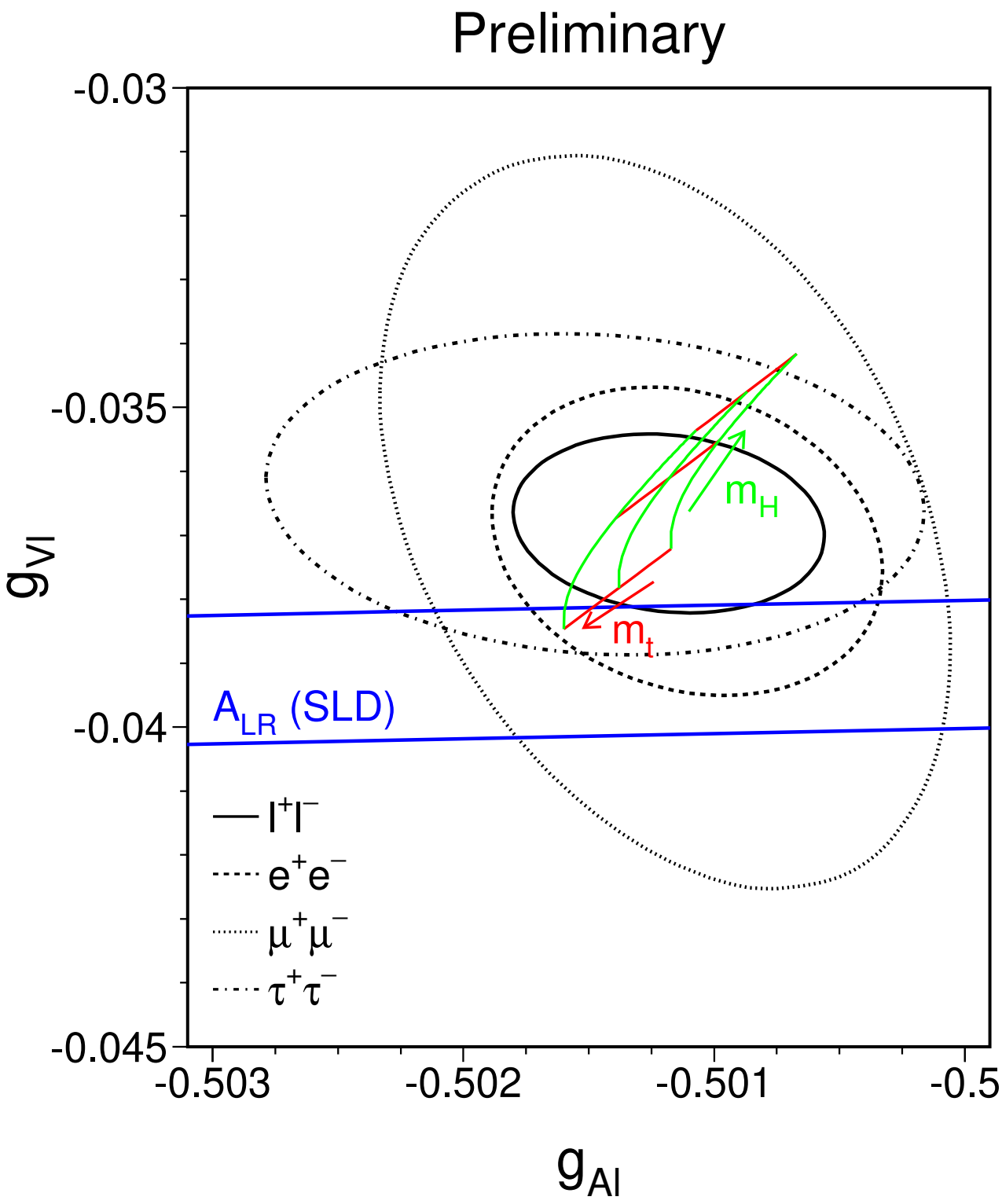

Figure 2: Contours of 68% probability in the $g_{V\ell}$-$g_{A\ell}$ plane from LEP measurements. The solid contour results from a fit assuming lepton universality. Also shown is the one standard deviation band resulting from the $A_{\rm LR}$ measurement of SLD. The grid corresponds to the Standard Model prediction for $m_{\rm t} = 175 \pm 9$ GeV and $m_{\rm H} = 300^{+700}_{-240}$ GeV. The arrows point in the direction of increasing values of $m_{\rm t}$ and $m_{\rm H}$.

6.3 The Effective Electroweak Mixing Angle $\sin^2\theta^{\rm lept}_{\rm eff}$

The asymmetry measurements from LEP can be combined into a single observable, the effective electroweak mixing angle, $\sin^2\theta^{\rm lept}_{\rm eff}$, defined as:

$$\sin^2\theta^{\rm lept}_{\rm eff} \equiv \frac{1}{4}(1 - g_{V\ell}/g_{A\ell})\,, \tag{13}$$

without making any strong model-specific assumptions.

For a combined average of $\sin^2\theta^{\rm lept}_{\rm eff}$ from $A^{0,\ell}_{\rm FB}$, $\mathcal{A}_\tau$ and $\mathcal{A}_{\rm e}$ only the assumption of lepton universality, already inherent in the definition of $\sin^2\theta^{\rm lept}_{\rm eff}$, is needed. In practice no further assumption is involved if the quark forward-backward asymmetries, $A^{\rm b\bar{b}}_{\rm FB}$ and $A^{\rm c\bar{c}}_{\rm FB}$, are included in this average, as these asymmetries have a reduced sensitivity to corrections particular to the hadronic vertex. The results of these determinations of $\sin^2\theta^{\rm lept}_{\rm eff}$ and their combination are shown in Table 21. Also the comparison with the measurement of the left-right asymmetry, $A_{\rm LR}$, from SLD [5,6] is given.

	$\sin^2\theta^{\rm lept}_{\rm eff}$	Average by Group of Observations	Cumulative Average	χ^2/d.o.f.
$A^{0,\ell}_{\rm FB}$	0.23103 ± 0.00062			
$\mathcal{A}_\tau$	0.23249 ± 0.00088			
$\mathcal{A}_{\rm e}$	0.23204 ± 0.00100	0.23162 ± 0.00045	0.23162 ± 0.00045	2.1/2
$A^{0,\rm b}_{\rm FB}$	0.23204 ± 0.00050			
$A^{0,\rm c}_{\rm FB}$	0.2311 ± 0.0012	0.23189 ± 0.00046	0.23176 ± 0.00032	2.8/4
$\langle Q_{\rm FB}\rangle$	0.2320 ± 0.0010	0.2320 ± 0.0010	0.23178 ± 0.00031	2.9/5
$A_{\rm LR}$ (SLD)	0.23049 ± 0.00050	0.23049 ± 0.00050	0.23143 ± 0.00026	7.7/6

Table 21: Comparison of several determinations of $\sin^2\theta^{\rm lept}_{\rm eff}$ from asymmetries. Averages are obtained as weighted averages assuming no correlations. The second column lists the $\sin^2\theta^{\rm lept}_{\rm eff}$ values derived from the quantities listed in the first column. The third column contains the averages of these numbers by groups of observations, where the groups are separated by the horizontal lines. The last column shows the cumulative averages. The χ^2 per degree of freedom for the cumulative averages is also given.

6.4 Number of Neutrino Species

An important aspect of our measurement concerns the information related to Z decays into invisible channels. Using the results of Tables 7 and 8, the ratio of the Z decay width into invisible particles and the leptonic decay width is determined:

$$\Gamma_{\rm inv}/\Gamma_{\ell\ell} \;=\; 5.954 \pm 0.031\,.$$

The Standard Model value for the ratio of the partial widths to neutrinos and charged leptons is:

$$(\Gamma_{\nu\nu}/\Gamma_{\ell\ell})_{\rm SM} \;=\; 1.991 \pm 0.001\,.$$

The central value is evaluated for $m_{\rm Z} = 91.1884$ GeV, $m_{\rm t} = 180$ GeV, $m_{\rm H} = 300$ GeV and the error quoted accounts for a variation of $m_{\rm t}$ in the range $m_{\rm t} = 175 \pm 9$ GeV and a variation of $m_{\rm H}$ in the range 60 GeV $\leq m_{\rm H} \leq$ 1000 GeV.

The number of light neutrino species is given by the ratio of the two expressions listed above:

$$N_\nu \;\; = \;\; 2.991 \pm 0.016\,.$$

6.5 Constraints on the Standard Model

The precise electroweak measurements performed at LEP can be used to check the validity of the Standard Model and, within its framework, to infer valuable information about its fundamental parameters. The accuracy of the measurements makes them sensitive to the top-quark mass, $m_{\rm t}$, and to the mass of the Higgs boson, $m_{\rm H}$, through loop corrections. The leading $m_{\rm t}$ dependence is quadratic and allows a determination of $m_{\rm t}$. The main dependence on $m_{\rm H}$ is logarithmic and therefore, with the present data accuracy, the constraints on $m_{\rm H}$ are still weak.

The various LEP measurements are summarized in Table 22a and are presented in Figures 3, 4 and 5, together with their Standard Model prediction as a function of $m_{\rm t}$. The bands in the Standard Model predictions reflect the linear sum of the expected variations in each quantity due to a change of the strong coupling constant $\alpha_s(m_{\rm Z}^2) = 0.123 \pm 0.006$ [57] and $m_{\rm H}$ in the interval 60 GeV $\leq m_{\rm H} \leq$ 1000 GeV for $m_{\rm Z} = 91.1884$ GeV.

Detailed studies of the theoretical uncertainties in the Standard Model predictions due to missing higher-order electroweak corrections and their interplay with QCD corrections are carried out in the working group on 'Precision calculations for the Z resonance' [58]. Theoretical uncertainties are evaluated by comparing different but, within our present knowledge, equivalent treatments of aspects such as resummation techniques, momentum transfer scales for vertex corrections and factorization schemes. The impact of these intrinsic theoretical uncertainties on $m_{\rm t}$ and $\alpha_s(m_{\rm Z}^2)$ has been estimated by repeating the Standard Model fits in this Section using several combinations of options which were implemented in the electroweak libraries used [59] for the study performed in [58]. As a result the maximal variations of the central values of the fitted parameters correspond to an additional theoretical error of less than 2 GeV on $m_{\rm t}$ and less than 0.001 on $\alpha_s(m_{\rm Z}^2)$. This error on $\alpha_s(m_{\rm Z}^2)$ covers missing higher-order electroweak corrections and uncertainties in the interplay of electroweak and QCD corrections but not the effect of missing higher-order QCD corrections. A discussion of theoretical uncertainties in the determination of α_s can be found in [58,60]. These theoretical errors have been neglected for the results presented in Table 23.

At present the impact of theoretical uncertainties on the determination of $m_{\rm t}$ from precise electroweak measurements is negligible compared to the error due to the uncertainty in the value of the fine structure constant $\alpha(m_{\rm Z}^2)$. The uncertainty in $\alpha(m_{\rm Z}^2)$ arises from the contribution of light quarks to the photon vacuum polarization. Recently there have been several reevaluations of $\alpha(m_{\rm Z}^2)$ [61–64]. For the results presented in this Section, a value of $\alpha(m_{\rm Z}^2) = 1/(128.896 \pm 0.090)$ [63] is used. This uncertainty causes an error of 0.00023 on the Standard Model prediction of $\sin^2\theta_{\rm eff}^{\rm lept}$ and an error of 4 GeV on $m_{\rm t}$, which are included in the results listed in Table 23. The effect on the Standard Model prediction for $\Gamma_{\ell\ell}$ is negligible. The $\alpha_s(m_{\rm Z}^2)$ values for the Standard Model fits presented in this Section are stable against a variation of $\alpha(m_{\rm Z}^2)$ in the interval quoted.

	Measurement with Total Error	Standard Model	Pull
a) LEP			
line-shape and lepton asymmetries:			
m_Z [GeV]	91.1884 ± 0.0022	91.1869	0.7
Γ_Z [GeV]	2.4964 ± 0.0032	2.4979	-0.5
σ_h^0 [nb]	41.490 ± 0.078	41.454	0.5
R_ℓ	20.788 ± 0.032	20.770	0.6
$A_{FB}^{0,\ell}$	0.0171 ± 0.0011	0.0159	1.1
+ correlation matrix Table 8			
τ polarization:			
$\mathcal{A}_\tau$	0.1394 ± 0.0069	0.1455	-0.9
$\mathcal{A}_e$	0.1429 ± 0.0079	0.1455	-0.3
b and c quark results:			
$R_b^{(b)}$	0.2215 ± 0.0017	0.2155	3.5
$R_c^{(b)}$	0.1596 ± 0.0070	0.1725	-1.8
$A_{FB}^{0,b(b)}$	0.1002 ± 0.0028	0.1020	-0.6
$A_{FB}^{0,c(b)}$	0.0756 ± 0.0051	0.0728	0.5
+ correlation matrix Table 15			
$q\bar{q}$ charge asymmetry:			
$\sin^2\theta_{eff}^{lept}$ ($\langle Q_{FB} \rangle$)	0.2320 ± 0.0010	0.23171	0.3
b) SLD			
$\sin^2\theta_{eff}^{lept}$ (A_{LR} [5,6])	0.23049 ± 0.00050	0.23172	-2.4
R_b [8]$^{(b)}$	0.2176 ± 0.0039	0.2155	0.5
$\mathcal{A}_b$ [7]	0.842 ± 0.052	0.934	-1.8
$\mathcal{A}_c$ [7]	0.618 ± 0.091	0.667	-0.5
c) $p\bar{p}$ and νN			
m_W [GeV] ($p\bar{p}$ [65])	80.33 ± 0.15	80.37	-0.2
$1 - m_W^2/m_Z^2$ (νN [9–11])	0.2257 ± 0.0047	0.2232	0.5

Table 22: Summary of measurements included in the combined analysis of Standard Model parameters. Section a) summarizes LEP averages, Section b) SLD results for $\sin^2\theta_{eff}^{lept}$ from the measurement of the left-right polarization asymmetry, for R_b and for $\mathcal{A}_b$ and $\mathcal{A}_c$ from polarized forward-backward asymmetries and Section c) electroweak precision measurements from $p\bar{p}$ colliders and νN scattering. The Standard Model results in column 2 and the pulls (difference between measurement and fit in units of the total measurement error) in column 3 are derived from the Standard Model fit including all data (Table 23, column 3) for a fixed value of $m_H = 300$ GeV.

$^{(a)}$The systematic errors on m_Z and Γ_Z contain the errors arising from the uncertainties in the LEP energy only.

$^{(b)}$For fits which combine LEP and SLD heavy flavour measurements we use as input the heavy flavour results given in Equation (11) and their correlation matrix in Table 16 in Section 4 of this note.

	LEP	LEP + SLD	LEP + SLD + $p\bar{p}$ and νN data
m_t (GeV)	$172\ ^{+9}_{-10}\ ^{+18}_{-20}$	$180\ ^{+8}_{-9}\ ^{+18}_{-21}$	$179 \pm 8\ ^{+18}_{-20}$
$\alpha_s(m_Z^2)$	$0.124 \pm 0.004 \pm 0.002$	$0.123 \pm 0.004 \pm 0.002$	$0.123 \pm 0.004 \pm 0.002$
χ^2/d.o.f.	15/9	24/12	25/14
$\sin^2\theta_{\rm eff}^{\rm lept}$	$0.23195 \pm 0.00026\ ^{+0.00007}_{-0.00014}$	$0.23163 \pm 0.00024\ ^{+0.00006}_{-0.00012}$	$0.23164 \pm 0.00022\ ^{+0.00007}_{-0.00010}$
$1 - m_W^2/m_Z^2$	$0.2244 \pm 0.0009\ ^{+0.0005}_{-0.0003}$	$0.2235 \pm 0.0008\ ^{+0.0005}_{-0.0004}$	$0.2236 \pm 0.0007\ ^{+0.0004}_{-0.0003}$
m_W (GeV)	$80.305 \pm 0.053\ ^{+0.016}_{-0.027}$	$80.357 \pm 0.046\ ^{+0.017}_{-0.029}$	$80.350 \pm 0.042\ ^{+0.016}_{-0.025}$

Table 23: Results of fits to LEP and other electroweak precision data for m_t and $\alpha_s(m_Z^2)$. No external constraint on $\alpha_s(m_Z^2)$ has been imposed. The first column presents the results obtained using LEP data only (Table 22a). The second column gives the result when the SLD measurements of the left-right asymmetry and electroweak heavy flavour results (Table 22b) are also added. In the third column also the combined data from $p\bar{p}$ colliders and νN experiments (Table 22c) are included. The central values and the first errors quoted refer to $m_H = 300$ GeV. The second errors correspond to the variation of the central value when varying m_H in the interval 60 GeV $\leq m_H \leq$ 1000 GeV. The bottom part of the table lists derived results for $\sin^2\theta_{\rm eff}^{\rm lept}$, $1 - m_W^2/m_Z^2$ and m_W.

Table 23 shows the constraints obtained on m_t and $\alpha_s(m_Z^2)$ when fitting the measurements in Table 22 to up-to-date Standard Model calculations [59]. The fits have been repeated for $m_H = 60$, 300 and 1000 GeV and the difference in the fitted parameters is quoted as the second uncertainty. The results obtained using only LEP data (Table 22a), as well as those obtained by including preliminary results from the SLD collaboration (Table 22b) for the left-right asymmetry, A_{LR} [5,6], and the measurements with heavy flavours (R_b [8], $\mathcal{A}_b$ and $\mathcal{A}_c$ [7]) are shown in Table 23. The right-most column of Table 23 gives the Standard Model constraints obtained by including in addition the published measurements of m_W from UA2 [12], CDF [13,14], a preliminary result for m_W from DØ [15][3], and the measurements of the neutrino neutral to charged current ratios from CDHS [9], CHARM [10] and CCFR [11] (Table 22c).

The χ^2/d.o.f. values for all these fits have probabilities ranging from 1.8% to 9.1%. The measurements of R_b and R_c, dominated by systematic errors, cause a χ^2 contribution of approximately 12 for all the Standard Model fits in Table 23 (see also Table 22). In the Standard Model the predictions of R_b and R_c are not very sensitive to m_t and $\alpha_s(m_Z^2)$ compared to other input data of this analysis. If they are omitted from the fit the fitted value of m_t increases by only 4 GeV, and the value of $\alpha_s(m_Z^2)$ stays approximately constant.

The fitted value of m_t is in excellent agreement with the top mass values $m_t = 175.7 \pm 5.7$ (stat.) $\pm$ 7.4 (syst.) GeV and $m_t = 170 \pm 15$ (stat.) $\pm$ 10 (syst.) GeV reported from the observation of the top quark at the TEVATRON by the CDF [16] and the DØ collaborations [17], respectively. For the sake of comparison with electroweak precision data the weighted average of both measurements, assuming 100% correlation of the smaller systematic error, $m_t = 175 \pm 9$ GeV, is used in this note.

As pointed out in Section 2, during 1995 drifts in the LEP energy were seen. Similar effects were presumably present in previous years, and could lead to a shift in the absolute energy scale of LEP, and thus to a shift in m_Z. Although unlikely, the measurement of Γ_Z could also be affected. For the

[3] See Reference 65 for a combination of these m_W measurements.

results of fits to all data (last column of Table 23), the effects are $dm_t/dm_Z = -0.22$ GeV/MeVand $dm_t/d\Gamma_Z = 1.2$ GeV/MeV. For the fits to LEP only data (first column of Table 23), the effect of m_Z is the same and that of Γ_Z increases to 1.6 GeV/MeV. The effect on $\alpha_s(m_Z^2)$ is $d\alpha_s(m_Z^2)/dm_Z = -0.00006$/MeVand $d\alpha_s(m_Z^2)/d\Gamma_Z = 0.0005$/MeV. It should be noted that quantities such as $A_{FB}^{0,\ell}$ (and hence $\sin^2\theta_{eff}^{lept}$) are unaffected by shifts in the LEP energy scale.

As shown above, the fitted values of m_t are insensitive to whether or not R_b and R_c are included in the fits. This is to be expected as the constraint on m_t comes mainly from the leptonic sector. Figure 6 shows a comparison of the leptonic partial width from LEP (Table 9) and the effective electroweak mixing angle from asymmetries measured at LEP and SLD (Table 21), with the Standard Model. Good agreement with the Standard Model prediction is observed. The star shows the prediction if, among the electroweak radiative corrections only the photon vacuum polarization is included, showing evidence that LEP/SLD data are sensitive to genuine electroweak corrections.

The value of $\alpha_s(m_Z^2)$ derived from an analysis of electroweak precision tests within the Standard Model framework depends essentially on R_ℓ, Γ_Z and σ_h^0. The result is in very good agreement with that obtained from event-shape measurements at LEP ($\alpha_s(m_Z^2) = 0.123 \pm 0.006$ [57]) and of similar precision. The strong coupling constant can also be determined from the parameter R_ℓ alone. For $m_Z = 91.1884$ GeV, and imposing $m_t = 175 \pm 9$ GeV as a constraint, $\alpha_s = 0.126 \pm 0.005 \pm 0.002$ is obtained, where the second error accounts for the variation of the result when varying m_H in the range 60 GeV $\leq m_H \leq$ 1000 GeV.

The averages of R_b and R_c (Table 22) have a strong correlation (-0.30). If the value of R_c is fixed to the Standard Model value $R_c = 0.172$, ignoring the pull of R_c, the agreement between the R_b result and the Standard Model fit result improves from 3.5 to 2.9 standard deviations. In this case one obtains $R_b = 0.2202 \pm 0.0016$. If this deviation of R_b is attributed to the b partial width, then R_ℓ should also be affected since $\Gamma_{b\bar{b}}$ is a component of the total hadronic width [66]. In Figure 7 the fitted result for R_b with R_c fixed to its Standard Model value is plotted versus $\sin^2\theta_{eff}^{lept}$. If one assumes the Standard Model dependence of the partial widths on $\sin^2\theta_{eff}^{lept}$ for the light quarks and the c quark, and takes $\alpha_s(m_Z^2) = 0.123 \pm 0.006$, R_ℓ imposes a constraint on the two variables. The one-sigma R_ℓ band is centred on the Standard Model prediction while the R_b band is off-set. The overlap, however, depends on the value of $\alpha_s(m_Z^2)$; it improves if the value of $\alpha_s(m_Z^2)$ is reduced. As mentioned above, the fitted value of $\alpha_s(m_Z^2)$ is insensitive to whether or not R_b and R_c are included in the fit. However, its value could vary widely depending on the interpretation given to the deviation of R_b and R_c.

Figure 8 shows the χ^2 value for the Standard Model fits discussed in Table 23 column 4, as a function of m_t for the three values of m_H (60, 300 and 1000 GeV) considered. It can be seen that the minima of these curves occur at different values of χ^2. This suggests the possibility of extracting constraints on the value of m_H.

The main m_H dependence of the Standard Model predictions for the measurements listed in Table 22 is given by corrections proportional to $\log(m_H)$. The effects of m_H and m_t, however, are correlated for most observables, which weakens the determination of m_H without a direct measurement of m_t. Figure 9 shows the observed value of $\Delta\chi^2 \equiv \chi^2 - \chi^2_{min}$ as a function of m_H, when the TEVATRON value of m_t is used as an additional constraint in the fit. The observed $\Delta\chi^2$ curve exhibits a minimum for low values of m_H. The $\Delta\chi^2 = 2.7$ interval, approximately corresponding to a 95% confidence level upper limit, extends up to 300 GeV (450 GeV) including (excluding) the measurements of R_b and R_c.

7 Conclusions

The combination of the many precise electroweak results yields stringent constraints on the Standard Model. All LEP measurements except two agree well with the predictions. The measurements of the ratios of the b and c quark partial widths of the Z to its total hadronic width, dominated by systematic errors, are in rather poor agreement with the Standard Model. This has only a small effect on the predicted top-quark mass, which is in good agreement with the direct measurement of the top mass at the TEVATRON. Including this direct measurement, the data show some sensitivity to the Higgs mass.

The LEP experiments wish to stress that this report reflects a preliminary status at the time of the 1996 winter conferences. A definitive statement on these results has to wait for publication by each collaboration.

Acknowledgments

We would like to thank the SL Division of CERN for the efficient operation of the LEP accelerator, the precise information on the absolute energy scale and their close cooperation with the four experiments. We would also like to thank members of the CCFR, CDF, DØ and SLD Collaborations for making results available to us in advance of the conferences and for useful discussions concerning their combination.

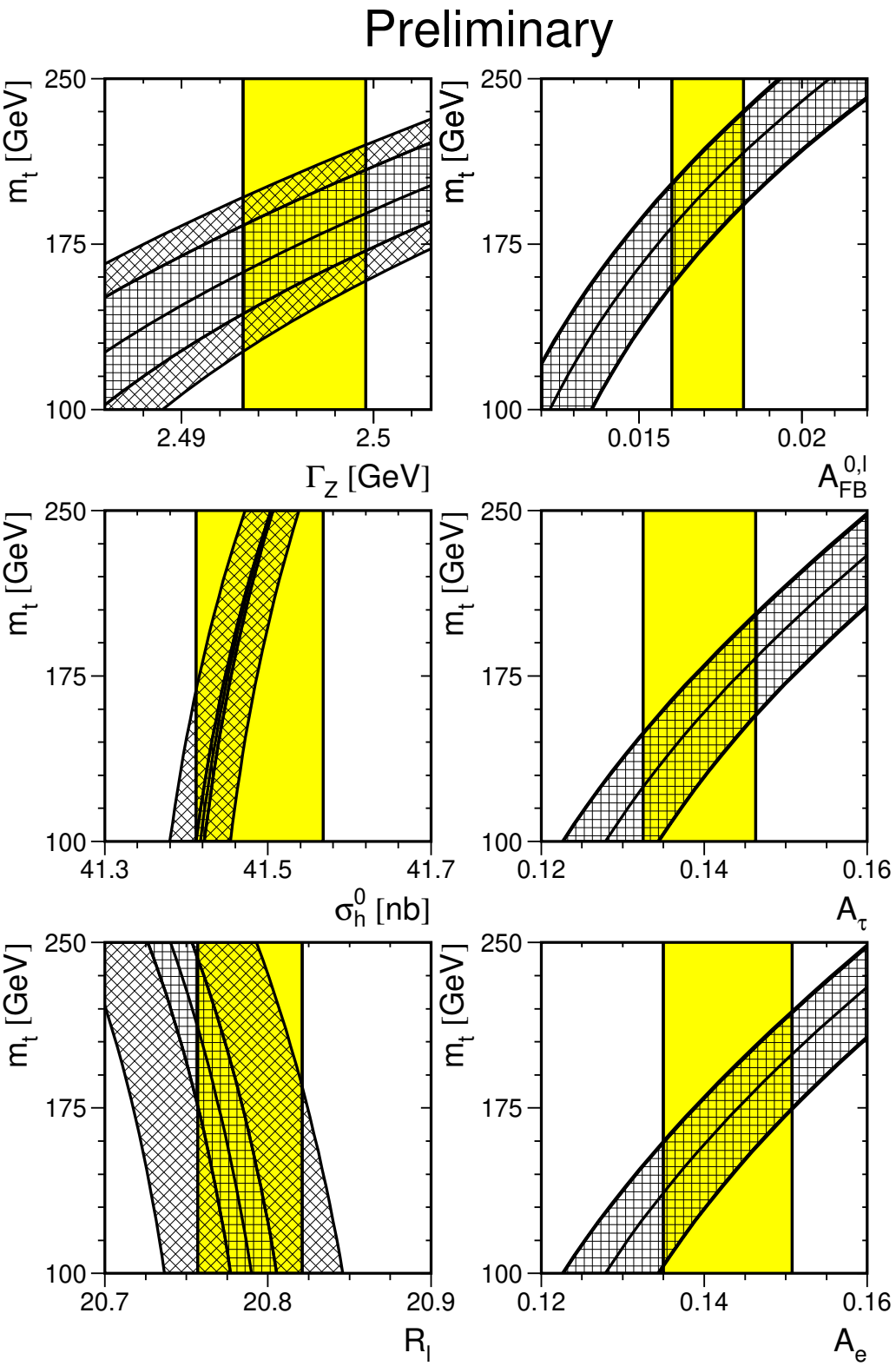

Figure 3: Comparison of LEP measurements with the Standard Model prediction as a function of m_t. The cross-hatch pattern parallel to the axes indicates the variation of the Standard Model prediction with m_H spanning the interval 60 GeV $\leq m_H \leq$ 1000 GeV, and the diagonal cross-hatch pattern corresponds to a variation of $\alpha_s(m_Z^2)$ within the interval $\alpha_s(m_Z^2) = 0.123 \pm 0.006$. The total width of the band corresponds to the linear sum of both uncertainties. The experimental errors on the parameters are indicated as vertical bands.

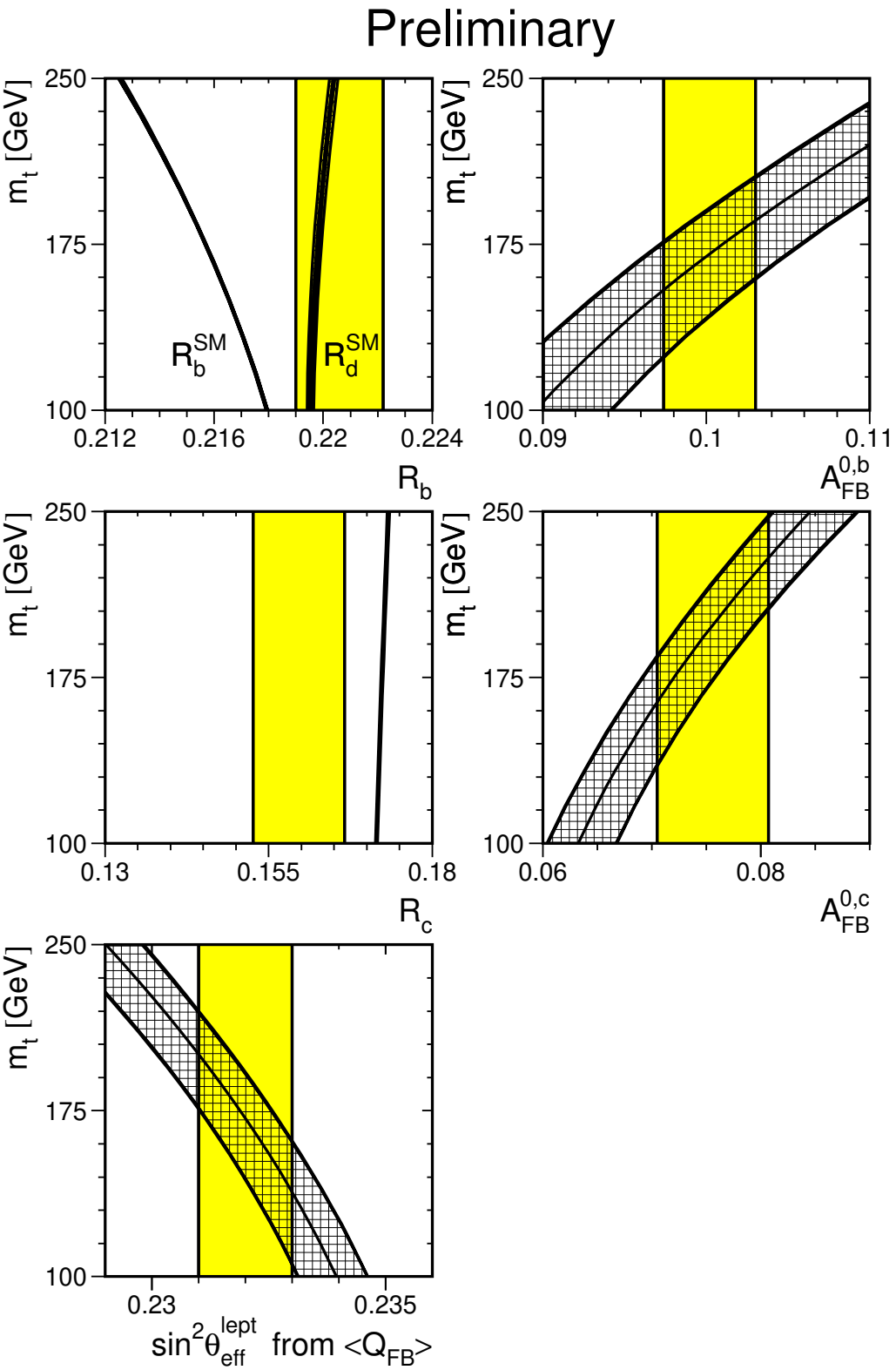

Figure 4: Comparison of LEP measurements with the Standard Model prediction as a function of m_{t} (*c.f.* Figure 3). For ratios of hadronic partial widths the variations with m_{H} and $\alpha_s(m_{\mathrm{Z}}^2)$ nearly cancel. For the comparison of R_{b} with the Standard Model the value of R_{c} has been fixed to its Standard Model prediction. To illustrate the impact of special vertex corrections to R_{b} the Standard Model prediction for R_{d} is also indicated.

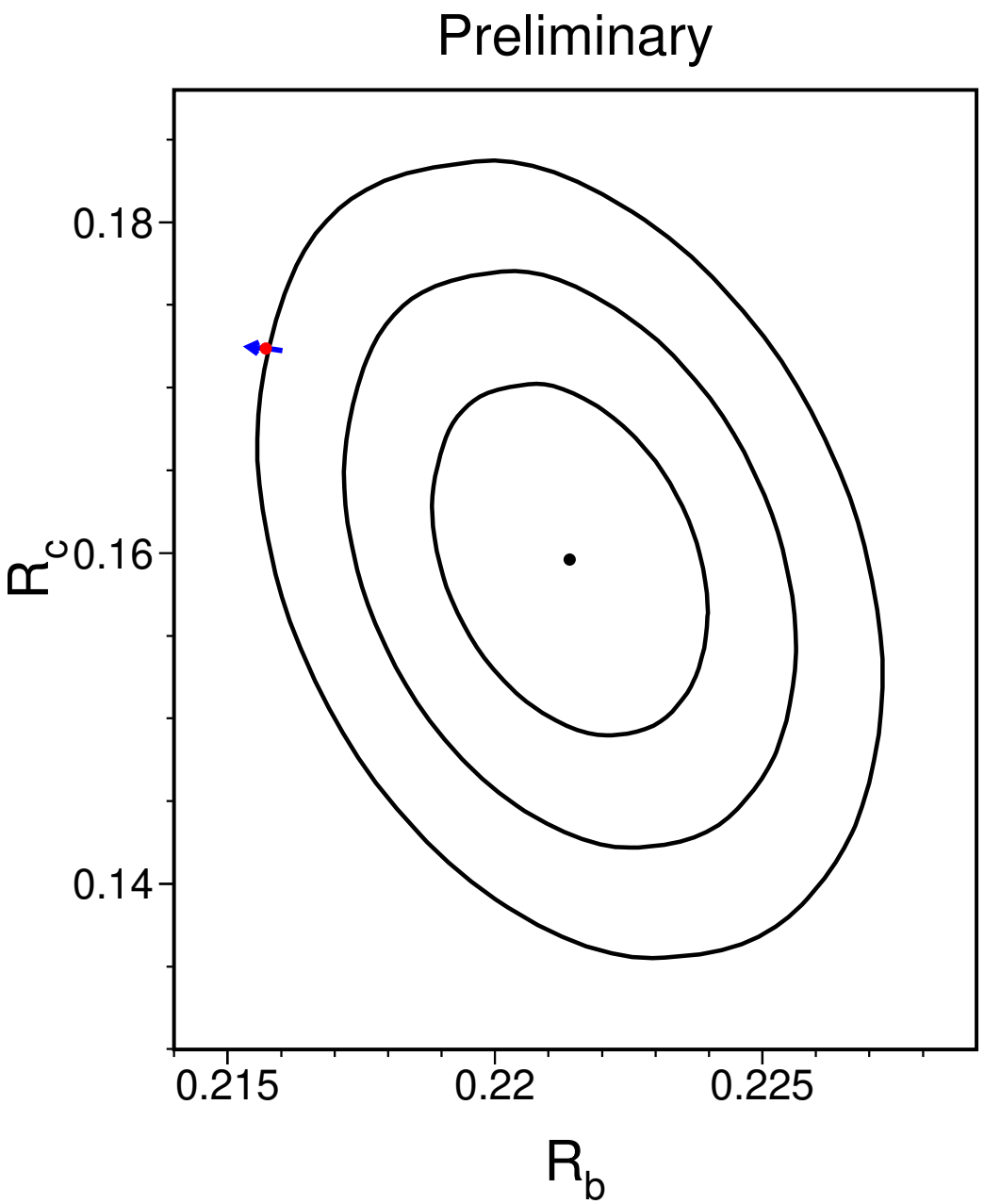

Figure 5: Contours in the R_b-R_c plane derived from LEP data, corresponding to 68%, 95% and 99.7% confidence levels assuming Gaussian systematic errors. The Standard Model prediction for $m_t = 175 \pm 9$ GeV is also shown. The arrow points in the direction of increasing values of m_t.

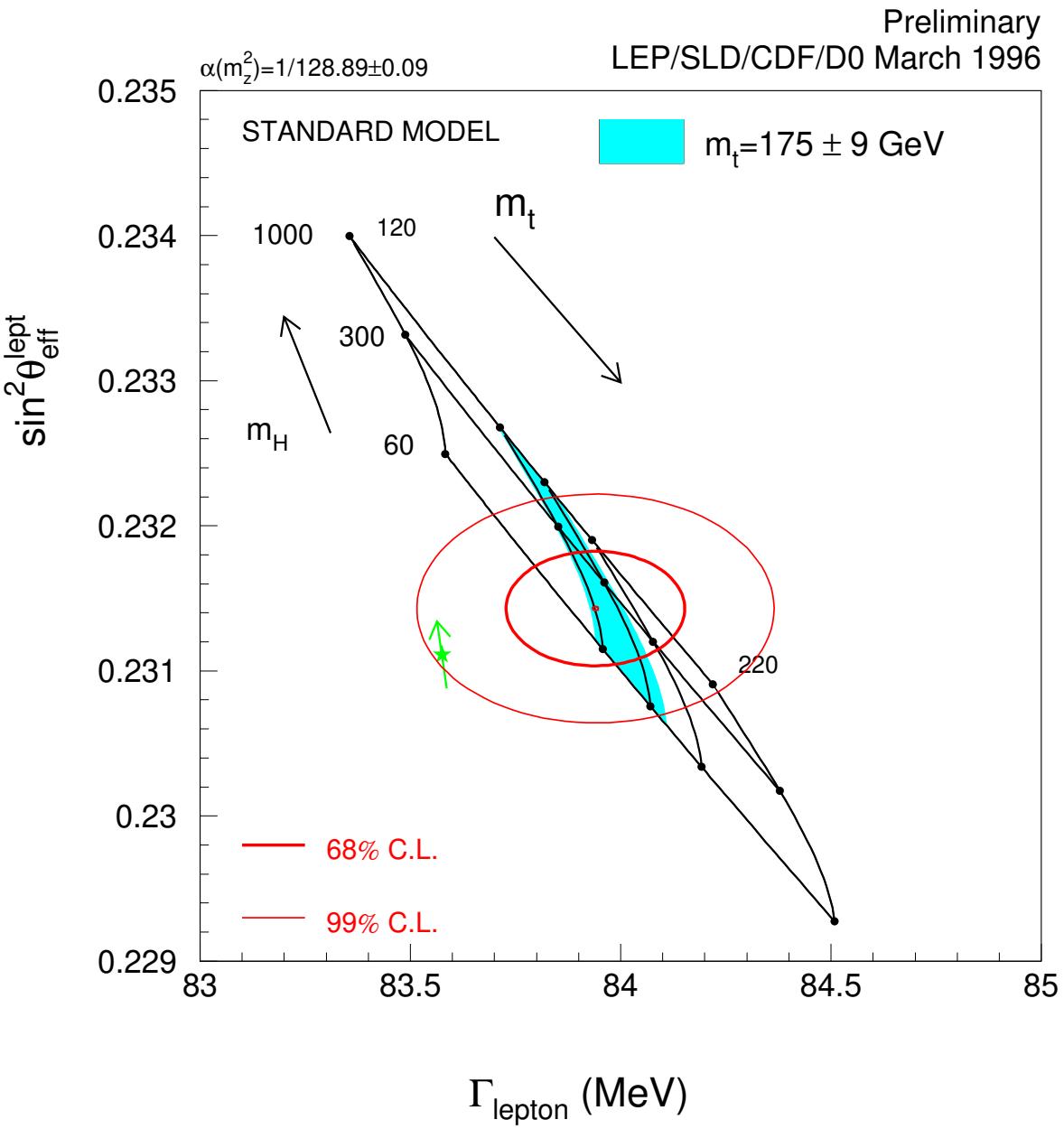

Figure 6: The LEP/SLD measurements of $\sin^2\theta^{\rm lept}_{\rm eff}$ (Table 21) and $\Gamma_{\ell\ell}$ (Table 9) and the Standard Model prediction. The star shows the predictions if among the electroweak radiative corrections only the photon vacuum polarization is included. The corresponding arrow shows variation of this prediction if $\alpha(m_{\rm Z}^2)$ is changing by one standard deviation. This variation gives an additional uncertainty to the Standard Model prediction shown in the figure.

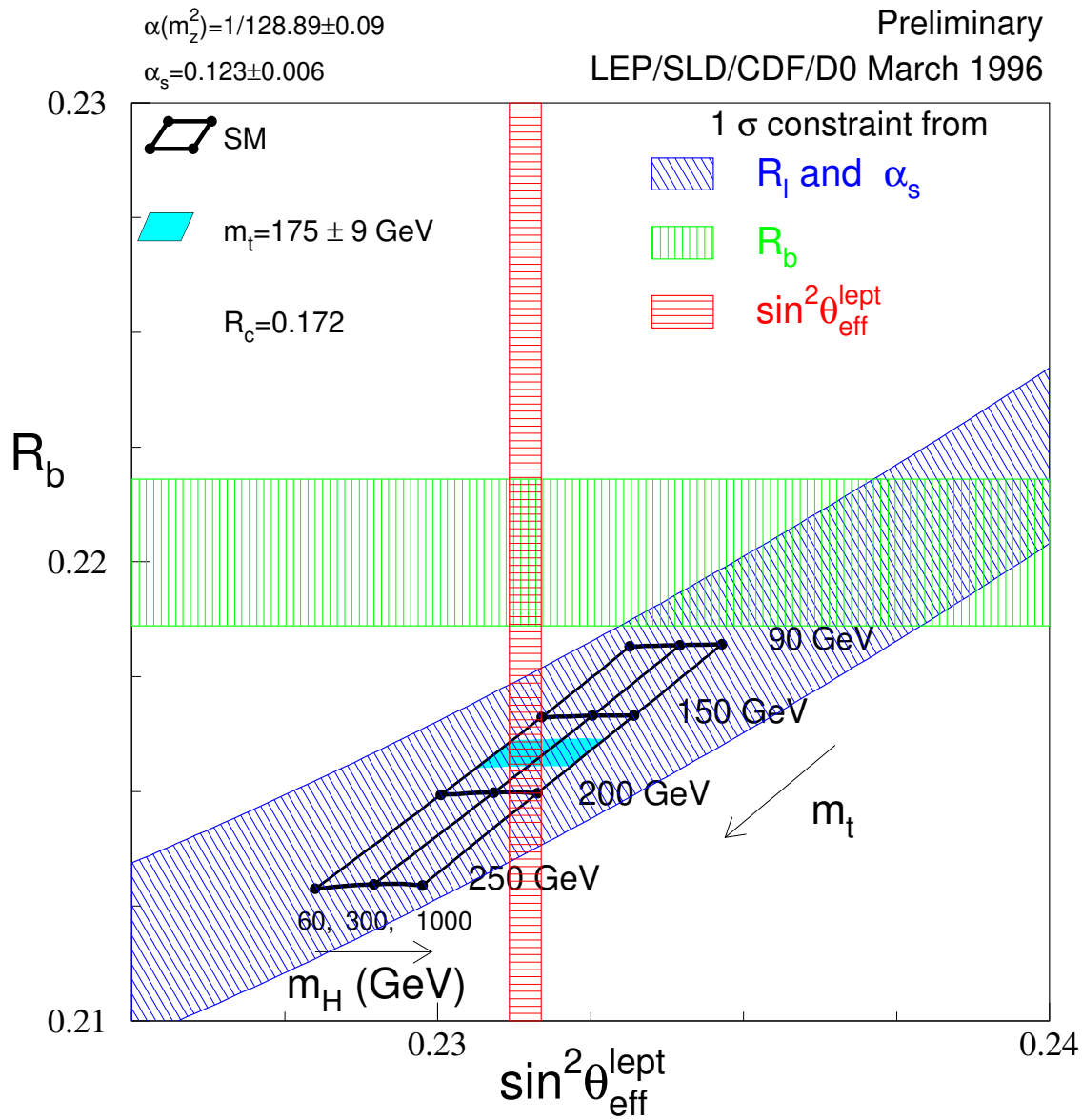

Figure 7: The LEP/SLD measurements of $\sin^2\theta^{\rm lept}_{\rm eff}$ (Table 21) and $R_{\rm b}(R_{\rm c} = 0.172)$ and the Standard Model prediction. Also shown is the constraint resulting from the measurement of R_ℓ on these variables, assuming $\alpha_s(m_{\rm Z}^2) = 0.123 \pm 0.006$, as well as the Standard Model dependence of light-quark partial widths on $\sin^2\theta^{\rm lept}_{\rm eff}$. The Standard Model value for $R_{\rm c}$ is assumed.

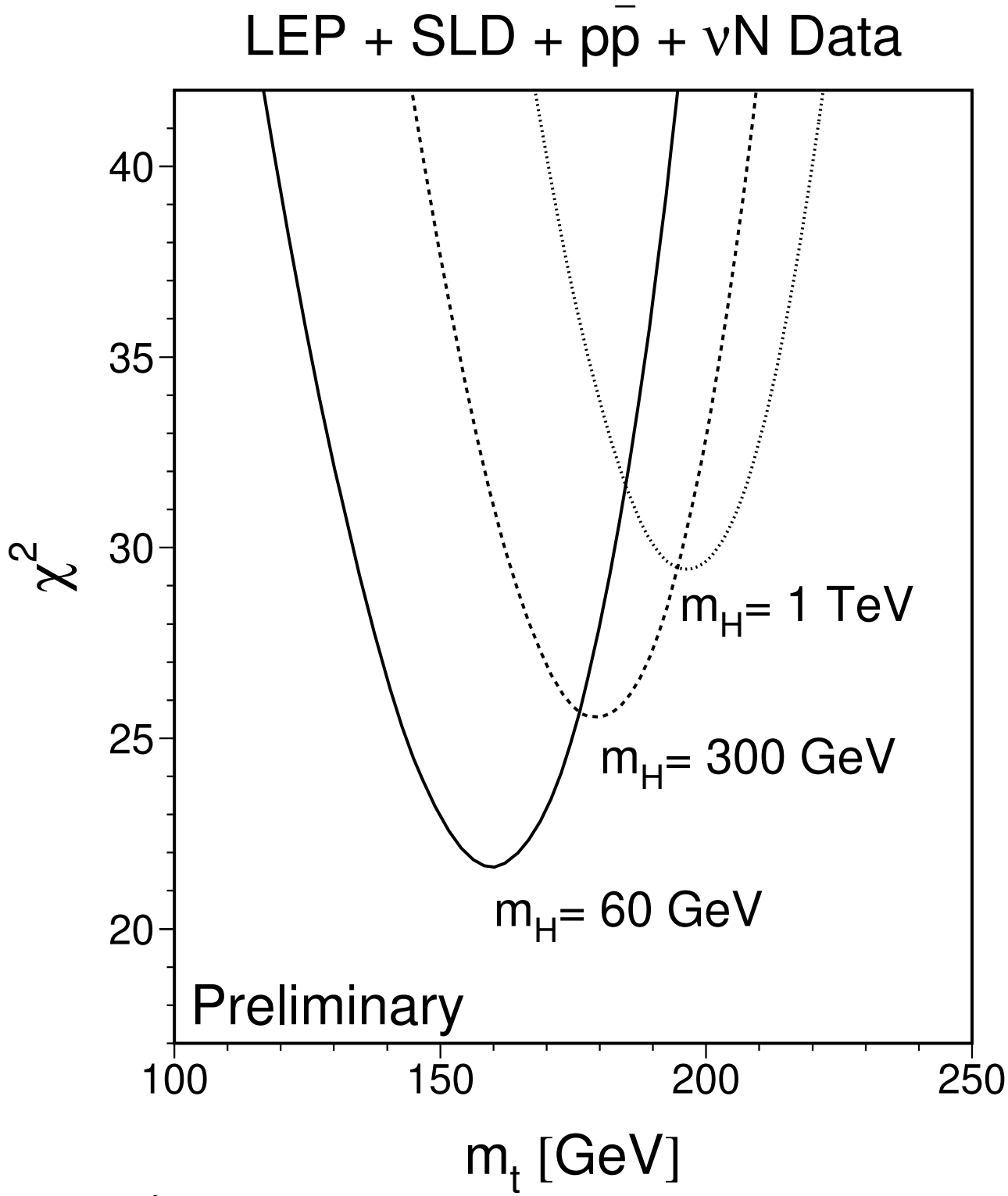

Figure 8: The χ^2 curves for the Standard Model fit in Table 23, column 4 to the electroweak precision measurements listed in Table 22 as a function of $m_{\rm t}$ for three different Higgs mass values spanning the interval 60 GeV $\leq m_{\rm H} \leq$ 1000 GeV.

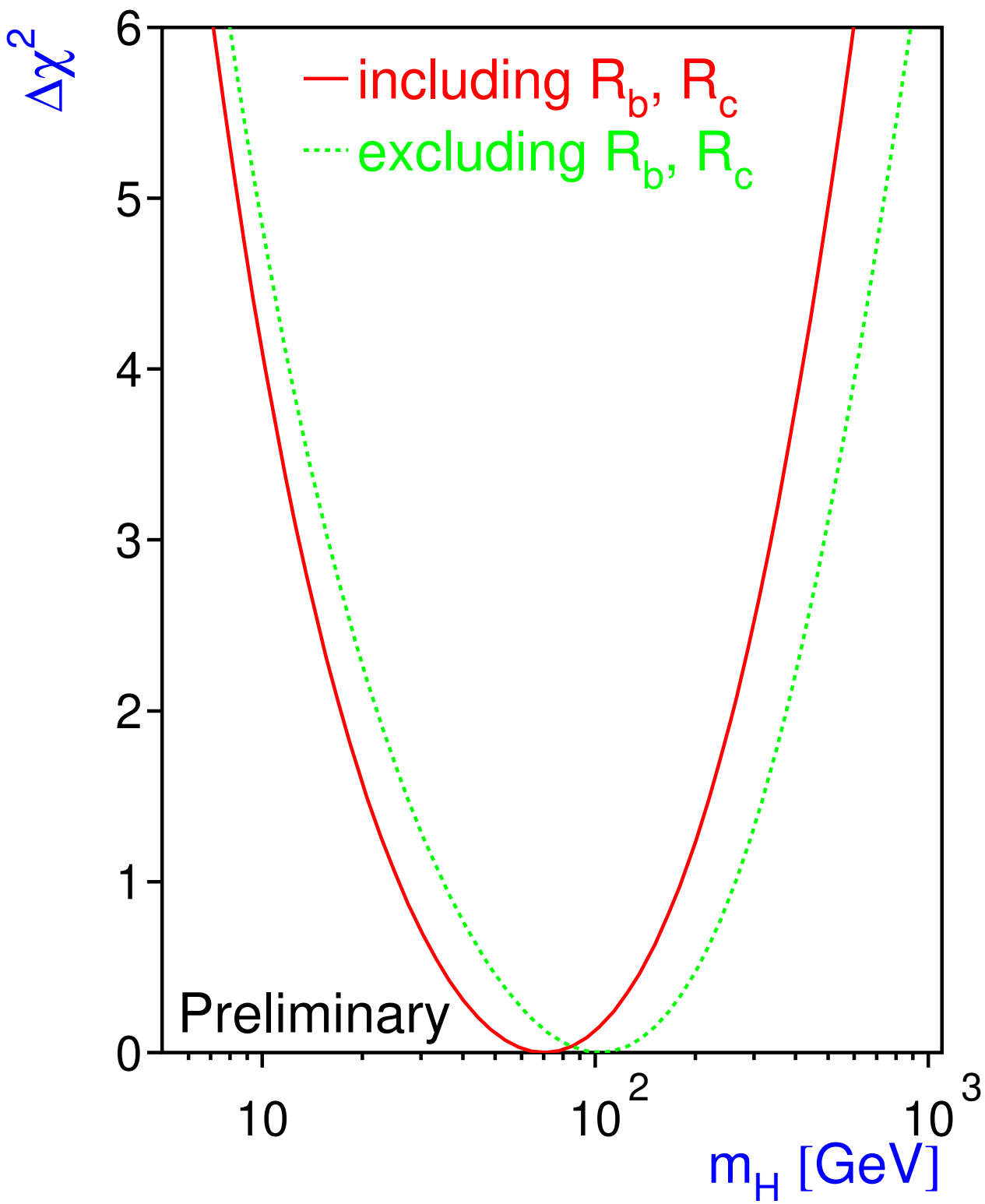

Figure 9: $\Delta\chi^2 = \chi^2 - \chi^2_{min}$ vs $m_{\rm H}$ curves. Continuous line: using all data (last column of Table 23); dashed line: as before, but excluding the LEP+SLD measurements of $R_{\rm b}$ and $R_{\rm c}$. In both cases, the direct measurement of $m_{\rm t}$ at the TEVATRON is included.

Appendix

Heavy Flavour fit including off peak asymmetries

The full 14 parameter fit to the LEP and SLD data gave the following results:

$$
\begin{aligned}
R_{\mathrm{b}} &= 0.2208 \pm 0.0016 \\
R_{\mathrm{c}} &= 0.1601 \pm 0.0070 \\
A_{\mathrm{FB}}^{\mathrm{b\bar{b}}}(-2) &= 0.059 \pm 0.012 \\
A_{\mathrm{FB}}^{\mathrm{c\bar{c}}}(-2) &= -0.044 \pm 0.024 \\
A_{\mathrm{FB}}^{\mathrm{b\bar{b}}}(\mathrm{pk}) &= 0.0947 \pm 0.0027 \\
A_{\mathrm{FB}}^{\mathrm{c\bar{c}}}(\mathrm{pk}) &= 0.0688 \pm 0.0053 \\
A_{\mathrm{FB}}^{\mathrm{b\bar{b}}}(+2) &= 0.111 \pm 0.010 \\
A_{\mathrm{FB}}^{\mathrm{c\bar{c}}}(+2) &= 0.116 \pm 0.020 \\
\mathcal{A}_{\mathrm{b}} &= 0.841 \pm 0.052 \\
\mathcal{A}_{\mathrm{c}} &= 0.619 \pm 0.091 \\
\mathrm{BR}(\mathrm{b} \to \ell) &= 0.1111 \pm 0.0023 \\
\mathrm{BR}(\mathrm{b} \to \mathrm{c} \to \bar{\ell}) &= 0.0781 \pm 0.0040 \\
\overline{\chi} &= 0.1220 \pm 0.0052 \\
\mathrm{P}(\mathrm{c} \to \mathrm{D}^{*+}) \times \mathrm{BR}(\mathrm{D}^{*+} \to \pi^{+}\mathrm{D}^{0}) &= 0.1681 \pm 0.0071
\end{aligned}
$$

with a χ^2/dof of $39/(76-16)$. The corresponding correlation matrix is given in Table 24.

	1) R_{b}	2) R_{c}	3) $A_{\mathrm{FB}}^{\mathrm{b\bar{b}}}(-2)$	4) $A_{\mathrm{FB}}^{\mathrm{c\bar{c}}}(-2)$	5) $A_{\mathrm{FB}}^{\mathrm{b\bar{b}}}$(pk)	6) $A_{\mathrm{FB}}^{\mathrm{c\bar{c}}}$(pk)	7) $A_{\mathrm{FB}}^{\mathrm{b\bar{b}}}(+2)$	8) $A_{\mathrm{FB}}^{\mathrm{c\bar{c}}}(+2)$	9) $\mathcal{A}_{\mathrm{b}}$	10) $\mathcal{A}_{\mathrm{c}}$	11) BR (1)	12) BR (2)	13) $\overline{\chi}$	14) PcDst
1)	1.00	−0.30	0.01	0.00	0.00	−0.03	0.00	−0.02	−0.06	0.05	−0.11	−0.07	0.06	0.10
2)	−0.30	1.00	0.00	0.00	0.05	0.02	0.01	0.02	0.07	−0.06	0.02	0.15	−0.03	−0.43
3)	0.01	0.00	1.00	0.11	0.03	0.01	0.02	0.00	0.00	0.02	0.03	−0.05	0.11	0.00
4)	0.00	0.00	0.11	1.00	0.01	0.01	0.00	0.00	0.00	0.00	0.00	−0.01	0.01	0.00
5)	0.00	0.05	0.03	0.01	1.00	0.09	0.07	0.00	0.04	−0.01	0.01	−0.13	0.25	−0.05
6)	−0.03	0.02	0.01	0.01	0.09	1.00	0.01	0.08	−0.01	0.06	−0.01	−0.06	0.07	0.01
7)	0.00	0.01	0.02	0.00	0.07	0.01	1.00	0.14	0.02	0.00	0.02	−0.07	0.14	−0.01
8)	−0.02	0.02	0.00	0.00	0.00	0.08	0.14	1.00	0.00	0.02	−0.01	−0.01	0.00	0.00
9)	−0.06	0.07	0.00	0.00	0.04	−0.01	0.02	0.00	1.00	0.07	0.00	−0.06	0.03	−0.03
10)	0.05	−0.06	0.02	0.00	−0.01	0.06	0.00	0.02	0.07	1.00	0.09	−0.13	0.15	0.01
11)	−0.11	0.02	0.03	0.00	0.01	−0.01	0.02	−0.01	0.00	0.09	1.00	−0.31	0.39	−0.01
12)	−0.07	0.15	−0.05	−0.01	−0.13	−0.06	−0.07	−0.01	−0.06	−0.13	−0.31	1.00	−0.46	−0.06
13)	0.06	−0.03	0.11	0.01	0.25	0.07	0.14	0.00	0.03	0.15	0.39	−0.46	1.00	0.00
14)	0.10	−0.43	0.00	0.00	−0.05	0.01	−0.01	0.00	−0.03	0.01	−0.01	−0.06	0.00	1.00

Table 24: The correlation matrix for the set of the 14 heavy flavour parameters. BR(1) and BR(2) denote $\mathrm{BR}(\mathrm{b} \to \ell)$ and $\mathrm{BR}(\mathrm{b} \to \mathrm{c} \to \bar{\ell})$ respectively, PcDst denotes $\mathrm{P}(\mathrm{c} \to \mathrm{D}^{*+}) \times \mathrm{BR}(\mathrm{D}^{*+} \to \pi^{+}\mathrm{D}^{0})$.

The Measurements used in the Heavy Flavour Averages

In the following tables, preliminary results are indicated by the symbol †. In each table, the values of centre-of-mass energy are given where relevant, followed by the result, the statistical error, the correlated and uncorrelated systematic errors, the total systematic error, and any dependence on other electroweak parameters. Contributions to the correlated systematic error are from any sources of error shared with one or more other results in the same table, and the uncorrelated errors from the remaining sources. Constants such as $a(x)$ denote the dependence on the assumed value of $x^{\rm used}$, which is also given.

	ALEPH			DELPHI	
Tagging	90-91 shape [34]	90-91 lepton [29]	92 lifetime [36]	90-93 multiple [37]	91-92 lepton [30]
$R_{\rm b}$	0.2280	0.2162	0.2187	0.2213	0.2145
Statistical	0.0054	0.0062	0.0022	0.0016	0.0089
Uncorrelated	0.0036	0.0028	0.0022	0.0013	0.0063
Correlated	0.0032	0.0042	0.0012	0.0016	0.0023
Total Systematic	0.0048	0.0050	0.0025	0.0021	0.0067
$a(R_{\rm c})$	-0.004		-0.014	-0.015	
$R_{\rm c}^{\rm used}$	0.165		0.172	0.171	

	L3		OPAL		SLD
Tagging	91 shape [35]	90-91† lepton [32]	92-94† multiple [38]	90-91 lepton [33]	93-94† lifetime [8]
$R_{\rm b}$	0.2220	0.2187	0.2197	0.2250	0.2176
Statistical	0.0030	0.0081	0.0014	0.0110	0.0032
Uncorrelated	0.0053	0.0047	0.0012	0.0035	0.0017
Correlated	0.0036	0.0034	0.0018	0.0057	0.0009
Total Systematic	0.0064	0.0058	0.0022	0.0066	0.0019
$a(R_{\rm c})$	-0.021	-0.023	-0.018	-0.013	-0.0093
$R_{\rm c}^{\rm used}$	0.171	0.171	0.171	0.171	0.171
$a({\rm BR(b}\to\ell))$	-0.001				
${\rm BR(b}\to\ell)^{\rm used}$ [%]	10.5				
$a({\rm BR(b}\to{\rm c}\to\ell))$		0.034			
${\rm BR(b}\to{\rm c}\to\bar{\ell})^{\rm used}$ [%]		7.9			

Table 25: The measurements of $R_{\rm b}$. There is an additional $+0.2$ statistical and $+0.2$ systematic correlation between the first two ALEPH results [29, 34].

	ALEPH	DELPHI			OPAL	
Tagging	90-91 lepton [29]	91-94† $D^{*\pm}$ incl./excl. [41]	91-93† D^0, D^+, D_s, Λ_c [41]	91-92 lepton [30]	90-94† $D^{*\pm}$ [42]	90-94† D^0, D^+, D_s, Λ_c [42]
R_c	0.1670	0.157	0.164	0.1625	0.150	0.166
Statistical	0.0054	0.006	0.011	0.0085	0.009	0.011
Uncorrelated	0.0149	0.009	0.009	0.0177	0.004	0.009
Correlated	0.0114	0.005	0.010	0.0111	0.011	0.012
Total Systematic	0.0188	0.010	0.013	0.0209	0.012	0.015

Table 26: The measurements of R_c.

	ALEPH			DELPHI		L3	OPAL		
Tagging	90-95† lepton [29]	90-95† lepton [29]	90-95† lepton [29]	91-94† lepton [31]	91-94† $D^{*\pm}$ [31]	90-93† lepton [32]	91-94 jet [40]	90-94 lepton [33]	90-94† $D^{*\pm}$ [44]
$\sqrt{s}$ (GeV)	88.38	89.38	90.21	89.43	89.54	89.56	89.52	89.52	89.54
$A_{FB}^{b\bar{b}}(-2)$	-3.5	5.3	8.6	6.3	1.9	7.02	6.3	5.6	2.7
Statistical	11.2	2.0	5.9	3.8	10.5	3.50	3.4	2.4	16.9
Uncorrelated	0.1	0.0	0.1	0.1	1.1	0.35	0.2	0.2	3.8
Correlated	0.2	0.0	0.1	0.1	0.8	0.12	0.1	0.2	0.3
Total Systematic	0.2	0.1	0.1	0.2	1.4	0.37	0.2	0.3	3.8
$a(R_b)$	1.09	-0.24	-0.85	−0.007		−1.642	−1.8	-0.004	
R_b^{used}	0.2192	0.2192	0.2192	0.217		0.216	0.216	0.2155	
$a(R_c)$	-0.90	0	0.60	0.122		0.913	0.01	0.003	
R_c^{used}	0.171	0.171	0.171	0.171		0.169	0.173	0.172	
$a(\overline{\chi})$	14.3	4.4	9.2	2.053					
$\overline{\chi}^{used}$	0.1268	0.1268	0.1268	0.121					
$a(BR(b \to \ell))$	1.1	-0.23	-0.85	−0.971		−0.928		1.0	
$BR(b \to \ell)^{used}$ [%]	11.34	11.34	11.34	11.0		10.5		10.9	
$a(BR(b \to c \to \bar{\ell}))$	0.04	-0.08	-0.24	0.158		−0.066		-1.6	
$BR(b \to c \to \bar{\ell})^{used}$ [%]	7.86	7.86	7.86	7.9		7.9		8.3	
$a(A_{FB}^{c\bar{c}}(-2))$	0.73	0.28	0.04			−0.267	−0.205		
$A_{FB}^{c\bar{c}}(-2)^{used}$	-0.0946	-0.0336	0.0055			−2.9	−3.16		

Table 27: The measurements of $A_{FB}^{b\bar{b}}(-2)$ (in units of 10^{-2}).

	ALEPH		DELPHI			L3	OPAL		
Tagging	90-95† lepton [29]	91-93 jet [39]	91-94† jet [31]	91-94† lepton [31]	91-94† $D^{*\pm}$ [31]	90-93† lepton [32]	91-94† jet [40]	90-94 lepton [33]	90-94† $D^{*\pm}$ [44]
$\sqrt{s}$ (GeV)	91.21	91.19	91.23	91.23	91.23	91.27	91.25	91.24	91.20
$A_{\rm FB}^{\rm b\bar{b}}(\rm pk)$	9.65	9.92	9.90	10.49	7.1	10.3	9.73	9.06	11.2
Statistical	0.45	0.84	0.72	0.76	2.5	1.0	0.67	0.51	3.5
Uncorrelated	0.10	0.25	0.28	0.19	1.1	0.4	0.23	0.14	1.7
Correlated	0.15	0.28	0.25	0.24	0.8	0.1	0.32	0.18	1.0
Total Systematic	0.17	0.38	0.38	0.31	1.4	0.4	0.39	0.23	2.0
$a(R_{\rm b})$	-1.34	-3.07	-0.6	-2.893		-1.642	-10.9	-0.009	
$R_{\rm b}^{\rm used}$	0.2192	0.2188	0.221	0.217		0.216	0.216	0.2155	
$a(R_{\rm c})$	1.03	$+2.57$	0.24	1.221		0.913	0.109	0.031	
$R_{\rm c}^{\rm used}$	0.171	0.171	0.171	0.171		0.169	0.173	0.172	
$a(\overline{\chi})$	3.34			3.447					
$\overline{\chi}^{\rm used}$	0.1268			0.121					
$a(\rm BR(b \to \ell))$	-1.30			-3.559		-0.647		-0.34	
$\rm BR(b \to \ell)^{used}$ [%]	11.34			11.0		10.5		10.9	
$a(\rm BR(b \to c \to \bar{\ell}))$	-0.20			0.474		-0.283		-0.53	
$\rm BR(b \to c \to \bar{\ell})^{used}$ [%]	7.86			7.9		7.9		8.3	
$a(A_{\rm FB}^{\rm c\bar{c}}(\rm pk))$	0.48					0.580	0.457		
$A_{\rm FB}^{\rm c\bar{c}}(\rm pk)^{\rm used}$	6.17					6.3	6.1		

Table 28: The measurements of $A_{\rm FB}^{\rm b\bar{b}}(\rm pk)$ (in units of 10^{-2}).

	ALEPH			DELPHI		L3	OPAL		
Tagging	90-95† lepton [29]	90-95† lepton [29]	90-95† lepton [29]	91-94† lepton [31]	91-94† $D^{*\pm}$ [31]	90-93† lepton [32]	91-94 jet [40]	90-94 lepton [33]	90-94† $D^{*\pm}$ [44]
$\sqrt{s}$ (GeV)	92.05	92.94	93.90	93.02	92.94	92.93	92.94	92.94	92.94
$A_{FB}^{b\bar{b}}(+2)$	3.8	10.3	8.8	14.9	5.6	11.0	17.3	11.7	−26.7
Statistical	5.1	1.6	8.8	3.6	9.6	2.9	2.9	2.0	14.0
Uncorrelated	0.1	0.2	0.1	0.5	1.1	0.4	0.6	0.2	4.0
Correlated	0.1	0.3	0.2	0.4	0.8	0.1	0.4	0.3	2.3
Total Systematic	0.2	0.4	0.3	0.6	1.4	0.4	0.7	0.3	4.6
$a(R_b)$	-1.0	-1.8	-1.7	−2.893		−1.642	−18.32	-0.015	
R_b^{used}	0.2192	0.2192	0.2192	0.217		0.216	0.216	0.2155	
$a(R_c)$	0.92	1.47	1.60	−0.977		0.913	0.157	0.061	
R_c^{used}	0.171	0.171	0.171	0.171		0.169	0.173	0.172	
$a(\overline{\chi})$	3.55	6.52	9.59	4.767					
$\overline{\chi}^{used}$	0.1268	0.1268	0.1268	0.121					
$a(BR(b \to \ell))$	-0.91	-1.76	-1.70	−3.235		−0.630		-1.0	
$BR(b \to \ell)^{used}$ [%]	11.34	11.34	11.34	11.0		10.5		10.9	
$a(BR(b \to c \to \bar{\ell}))$	-0.12	-0.23	-0.28	0.474		−0.303		-0.35	
$BR(b \to c \to \bar{\ell})^{used}$ [%]	7.86	7.86	7.86	7.9		7.9		8.3	
$a(A_{FB}^{c\bar{c}}(+2))$	0.75	0.97	0.85			1.113	0.840		
$A_{FB}^{c\bar{c}}(+2)^{used}$	9.72	12.51	14.78			12.1	12.0		

Table 29: The measurements of $A_{FB}^{b\bar{b}}(+2)$ (in units of 10^{-2}).

	ALEPH	DELPHI	OPAL	
Tagging	91-94† $D^{*\pm}$ [43]	91-94† $D^{*\pm}$ [31]	90-94 lepton [33]	91-94† $D^{*\pm}$ [44]
$\sqrt{s}$ (GeV)	89.4	89.54	89.52	89.54
$A_{FB}^{c\bar{c}}(-2)$	−4.9	0.2	-7.5	−0.6
Statistical	7.6	5.2	3.4	6.8
Uncorrelated	0.8	0.6	0.5	1.2
Correlated	0.0	0.1	0.3	0.1
Total Systematic	0.8	0.6	0.5	1.2
$a(A_{FB}^{b\bar{b}}(-2))$	0.291			
$A_{FB}^{b\bar{b}}(-2)^{used}$	−1.7			

Table 30: The measurements of $A_{FB}^{c\bar{c}}(-2)$ (in units of 10^{-2}).

	ALEPH		DELPHI		L3	OPAL	
Tagging	90-91 lepton [29]	91-94† $D^{*\pm}$ [43]	91-94† lepton [31]	91-94† $D^{*\pm}$ [31]	90-91 lepton [32]	90-94 lepton [33]	90-94† $D^{*\pm}$ [44]
$\sqrt{s}$ (GeV)	91.26	91.2	91.23	91.23	91.24	91.24	91.20
$A_{FB}^{c\bar{c}}(pk)$	9.1	6.4	8.37	7.5	7.8	6.00	6.8
Statistical	2.0	1.3	1.39	1.2	3.7	0.67	1.4
Uncorrelated	1.5	0.2	0.91	0.6	2.4	0.36	0.7
Correlated	1.0	0.2	0.74	0.1	0.6	0.36	0.1
Total Systematic	1.9	0.3	1.18	0.6	2.5	0.51	0.7
$a(R_b)$			3.617		4.32	0.009	
R_b^{used}			0.217		0.216	0.2155	
$a(R_c)$			−6.351		−6.76	-0.030	
R_c^{used}			0.171		0.169	0.172	
$a(BR(b \to \ell))$			4.853		3.501	3.75	
$BR(b \to \ell)^{used}$ [%]			11.0		10.5	10.9	
$a(BR(b \to c \to \bar{\ell}))$			−3.792		−0.303	-1.06	
$BR(b \to c \to \bar{\ell})^{used}$ [%]			7.9		7.9	8.3	
$a(A_{FB}^{b\bar{b}}(pk))$		−1.491			6.400		
$A_{FB}^{b\bar{b}}(pk)^{used}$		8.7			8.8		

Table 31: The measurements of $A_{FB}^{c\bar{c}}(pk)$ from D^* meson and lepton-tag analyses (in units of 10^{-2}).

	ALEPH	DELPHI	OPAL	
Tagging	91-94† $D^{*\pm}$ [43]	91-94† $D^{*\pm}$ [31]	90-94 lepton [33]	90-94† $D^{*\pm}$ [44]
$\sqrt{s}$ (GeV)	93.0	92.94	92.94	92.94
$A_{FB}^{c\bar{c}}(+2)$	10.9	8.0	14.1	17.1
Statistical	6.1	4.6	2.8	5.8
Uncorrelated	0.7	0.6	0.6	1.4
Correlated	0.3	0.1	0.6	0.1
Total Systematic	0.8	0.6	0.9	1.4
$a(A_{FB}^{b\bar{b}}(+2))$	−2.074			
$A_{FB}^{b\bar{b}}(+2)^{used}$	12.1			

Table 32: The measurements of $A_{FB}^{c\bar{c}}(+2)$ (in units of 10^{-2}).

	SLD		
Tagging	93-95† jet [7]	94-95† $K^{\pm}$ [7]	93-95† lepton [7]
$\sqrt{s}$ (GeV)	91.26	91.26	91.26
$\mathcal{A}_b$	0.843	0.907	0.865
Statistical	0.046	0.094	0.072
Uncorrelated	0.045	0.091	0.071
Correlated	0.020	0.013	0.017
Total Systematic	0.049	0.092	0.073
$a(R_b)$	−0.131	−0.022	−0.654
R_b^{used}	0.2180	0.2180	0.2180
$a(R_c)$	0.133	0.003	0.073
R_c^{used}	0.171	0.171	0.171
$a(\mathcal{A}_c)$	0.081	−0.133	
$\mathcal{A}_c{}^{used}$	0.666	0.666	
$a(\overline{\chi})$		0.223	0.020
$\overline{\chi}^{used}$		0.13	0.120
$a(BR(b \to \ell))$			−0.222
$BR(b \to \ell)^{used}$ [%]			10.8
$a(BR(b \to c \to \bar{\ell})$			0.064
$BR(b \to c \to \bar{\ell})^{used}$ [%]			9.3

Table 33: The measurements of $\mathcal{A}_b$.

	SLD	
Tagging	93-95† $D^{*\pm}$ [7]	93-95† lepton [7]
$\sqrt{s}$ (GeV)	91.26	91.26
$\mathcal{A}_c$	0.64	0.44
Statistical	0.11	0.11
Uncorrelated	0.05	0.08
Correlated	0.02	0.05
Total Systematic	0.06	0.10
$a(R_b)$		0.654
R_b^{used}		0.2180
$a(R_c)$		−0.452
R_c^{used}		0.171
$a(\mathcal{A}_b)$	−0.128	
$\mathcal{A}_b{}^{used}$	0.935	
$a(BR(b \to \ell))$		0.415
$BR(b \to \ell)^{used}$ [%]		10.8
$a(BR(b \to c \to \bar{\ell})$		−0.436
$BR(b \to c \to \bar{\ell})^{used}$ [%]		9.3

Table 34: The measurements of $\mathcal{A}_c$.

Tagging	ALEPH 90-91 lepton [29]	ALEPH 92-93† multiple [29]	DELPHI 91-92 lepton [30]	L3 90-91† lepton [32]	OPAL 90-91† lepton [33]
BR(b $\to \ell$)(%)	11.20	11.01	11.21	11.44	10.50
Statistical	0.33	0.10	0.45	0.48	0.60
Uncorrelated	0.32	0.20	0.50	0.37	0.39
Correlated	0.27	0.21	0.48	0.22	0.54
Total Systematic	0.42	0.29	0.70	0.43	0.66
$a(R_c)$				0.611	0.224
$R_c^{\rm used}$				0.171	0.171
$a(\overline{\chi})$		0.208			
$\overline{\chi}^{\rm used}$		0.1261			
a(BR(b $\to$ c $\to \bar{\ell}$)				0.461	
BR(b $\to$ c $\to \bar{\ell})^{\rm used}$ [%]				7.9	

Table 35: The measurements of BR(b $\to \ell$) from the lepton-tag analyses.

Tagging	ALEPH 90-91 lepton [29]	ALEPH 92-93† multiple [29]	DELPHI 91-92 lepton [30]	OPAL 90-91† lepton [33]
BR(b $\to$ c $\to \bar{\ell}$) (%)	8.81	7.68	7.70	8.30
Statistical	0.25	0.18	0.49	0.40
Uncorrelated	0.40	0.25	0.95	0.57
Correlated	0.69	0.42	0.83	0.39
Total Systematic	0.80	0.49	1.26	0.69
$a(R_c)$				0.316
$R_c^{\rm used}$				0.171
$a(\overline{\chi})$		-0.511		
$\overline{\chi}^{\rm used}$		0.1261		

Table 36: The measurements of BR(b $\to$ c $\to \bar{\ell}$) from the lepton-tag analyses.

Tagging	ALEPH 90-95† lepton [29]	DELPHI 91-92 lepton [30]	L3 90-93† lepton [32]	OPAL 90-94† lepton [33]
$\overline{\chi}$	0.12684	0.1500	0.1253	0.1107
Statistical	0.00512	0.0200	0.0110	0.0062
Uncorrelated	0.0023	0.0107	0.0053	0.0032
Correlated	0.0051	0.0119	0.0025	0.0038
Total Systematic	0.0058	0.0160	0.0058	0.0044
$a(R_{\mathrm{b}})$			0.001	0.032
$R_{\mathrm{b}}^{\mathrm{used}}$			0.216	0.2192
$a(R_{\mathrm{c}})$			0.001	
$R_{\mathrm{c}}^{\mathrm{used}}$			0.169	
$a(\mathrm{BR}(\mathrm{b} \to \ell))$			0.046	0.050
$\mathrm{BR}(\mathrm{b} \to \ell)^{\mathrm{used}}$ [%]			10.5	11.34
$a(\mathrm{BR}(\mathrm{b} \to \mathrm{c} \to \bar{\ell})$			−0.0342	-0.042
$\mathrm{BR}(\mathrm{b} \to \mathrm{c} \to \bar{\ell})^{\mathrm{used}}$ [%]			7.9	7.86

Table 37: The measurements of $\overline{\chi}$ from the lepton-tag analyses.

	DELPHI	OPAL
Tagging	91-94† $\mathrm{D}^{*\pm}$ [41]	90-94† $\mathrm{D}^{*\pm}$ [42]
$\mathrm{P}(\mathrm{c} \to \mathrm{D}^{*+}) \times \mathrm{BR}(\mathrm{D}^{*+} \to \pi^{+}\mathrm{D}^{0})$	0.1653	0.1685
Statistical	0.0086	0.0142
Uncorrelated	0.0072	0.0094
Correlated	0.0067	0.0035
Total Systematic	0.0098	0.0100

Table 38: The measurements of $\mathrm{P}(\mathrm{c} \to \mathrm{D}^{*+}) \times \mathrm{BR}(\mathrm{D}^{*+} \to \pi^{+}\mathrm{D}^{0})$.

References

[1] The LEP Collaborations ALEPH, DELPHI, L3, OPAL and the LEP Electroweak Working Group, *A Combination of Preliminary LEP Electroweak Measurements and Constraints on the Standard Model*, CERN-PPE/95-172.

[2] LEP Electroweak Working Group, *An Investigation of the Interference between Photon and Z-Boson Exchange*, Internal Note, LEPEWWG/LS/96-01, ALEPH 96-044 PHYSIC 96-040, DELPHI 96-40 PHYS 612, L3 Note 1926, OPAL Technical Note TN 359, ?? March 1996.

[3] The LEP Collaborations ALEPH, DELPHI, L3, OPAL and the LEP Electroweak Working Group, *Combined Preliminary Data on* Z *Parameters from the LEP Experiments and Constraints on the Standard Model*, CERN-PPE/94-187.

[4] The LEP Experiments, *Combining Heavy Flavour Electroweak Measurements at LEP* CERN–PPE/96–17, subm. to Nucl. Inst. Meth.

[5] SLD Collaboration, K. Abe *et al.*, Phys. Rev. Lett **73** (1994) 25.

[6] M. Woods, *The SLD* $A_{\rm LR}$ *Result and Review of Weak Mixing Angle Results at LEP and SLC*, Talk given at the EPS-HEP-95 Conference, Brussels, to appear in the Proceedings.

[7] J. Huber, *Left-right Forward-backward Asymmetry for c and b Quarks*, Talk given at the EPS-HEP-95 Conference, Brussels, to appear in the Proceedings;
C. Prescott, *Physics results with polarized electrons from SLAC*, Talk given at the 17th International Symposium on Lepton-Photon Interactions, 10-15/8/1995, Beijing, China, to appear in the Proceedings.

[8] SLD Collaboration, *Measurement of* R_b *at SLD*, Talk presented by Erez Etzion at Moriond QCD, 1996.

[9] CDHS Collaboration, H. Abramowicz *et al.*, Phys. Rev. Lett. **57** (1986) 298;
CDHS Collaboration, A. Blondel *et al.*, Z. Phys. **C45** (1990) 361.

[10] CHARM Collaboration, J.V. Allaby *et al.*, Phys. Lett. **B177** (1986) 446;
CHARM Collaboration, J.V. Allaby *et al.*, Z. Phys.**C36** (1987) 611.

[11] CCFR Collaboration, C.G. Arroyo *et al.*, Phys. Rev. Lett. **72** (1994) 3452;
D. Harris, *CCFR Measurement of* R_ν *and a New Extraction of* $\sin^2\theta_W$, Talk given at the EPS-HEP-95 Conference, Brussels, to appear in the Proceedings.

[12] UA2 Collaboration, J. Alitti *et al.*, Phys. Lett. **B276** (1992) 354.

[13] CDF Collaboration, F. Abe *et al.*, Phys. Rev. Lett. **65** (1990) 2243 and Phys. Rev. **D43** (1991) 2070.

[14] CDF Collaboration, F. Abe *et al.*, *Measurement of the W Boson Mass*, FERMILAB-PUB-95/033-E and FERMILAB-PUB-95/035-1995.

[15] DØ Collaboration, preliminary result presented by U. Heintz, Les Rencontres de Physique de la Vallee d'Aoste, La Thuile, March 1996.

[16] CDF Collaboration, A. Caner, presented at Les Rencontres de Physique de la Vallee d'Aoste, La Thuile, March 1996.

[17] DØ Collaboration, M. Narain, presented at Les Rencontres de Physique de la Vallee d'Aoste, La Thuile, March 1996.

[18] ALEPH Collaboration, D. Decamp *et al.*, Z. Phys. **C48** (1990) 365;
ALEPH Collaboration, D. Decamp *et al.*, Z. Phys. **C53** (1992) 1;
ALEPH Collaboration, D. Buskulic *et al.*, Z. Phys. **C60** (1993) 71;
ALEPH Collaboration, D. Buskulic *et al.*, Z. Phys. **C62** (1994) 539;
ALEPH Collaboration, *Preliminary Results on Z Production Cross Section and Lepton Forward-Backward Asymmetries using the 1994 Data*, note ALEPH 95-084 PHYSIC 95-078, eps0398.

[19] DELPHI Collaboration, P. Aarnio *et al.*, Nucl. Phys. **B367** (1991) 511;
DELPHI Collaboration, P. Abreu *et al.*, Nucl. Phys. **B417** (1994) 3;
DELPHI Collaboration, P. Abreu *et al.*, Nucl. Phys. **B418** (1994) 403;
DELPHI Collaboration, DELPHI Note 95-62 PHYS 497, July 1995;
DELPHI Collaboration, DELPHI Note 96-29 PHYS 603, March 1996.

[20] L3 Collaboration, B. Adeva *et al.*, Z. Phys. **C51** (1991) 179;
L3 Collaboration, O. Adriani *et al.*, Phys. Rep. **236** (1993) 1;
L3 Collaboration, M. Acciarri *et al.*, Z. Phys. **C62** (1994) 551;
L3 Collaboration, L3 Electroweak Update for 1995 Brussels/Beijing, L3 Note 1809, July 14, 1995.

[21] OPAL Collaboration, G. Alexander *et al.*, Z. Phys. **C52** (1991) 175;
OPAL Collaboration, P.D. Acton *et al.*, Z. Phys. **C58** (1993) 219;
OPAL Collaboration, R. Akers *et al.*, Z. Phys. **C61** (1994) 19;
OPAL Collaboration, *A Preliminary Update of the* Z *Line Shape and Lepton Asymmetry Measurements with the 1993 and 1994 Data*, Contributed Paper to EPS-HEP-95 Brussels, **eps0292**;
OPAL Collaboration, *The Preliminary OPAL SiW luminosity analysis: Results for the 1994 Summer conferences*, OPAL Physics Note PN142, July 1994.

[22] The LEP Collaborations ALEPH, DELPHI, L3, OPAL and the LEP Electroweak Working Group, *Updated Parameters of the* Z *Resonance from Combined Preliminary Data of the LEP Experiments*, CERN-PPE/93-157.

[23] See, for example, M. Consoli *et al.*, in "Z Physics at LEP 1", CERN Report CERN 89-08 (1989), eds G. Altarelli, R. Kleiss and C. Verzegnassi, Vol. 1, p. 7.

[24] The working group on LEP energy, R. Assmann et al., Z. Phys. **C66** (1995) 567.

[25] ALEPH Collaboration, D. Buskulic *et al.*, *Improved tau polarisation measurements*, CERN-PPE/95-023 (1995).

[26] DELPHI Collaboration, P. Abreu *et al.*, Z. Phys. **C67** (1995) 183.

[27] L3 Collaboration, O. Acciari *et al.*, Phys. Lett. **B341** (1994) 245;
L3 Collaboration, *A Preliminary Update of* A_τ *and* A_e *Using 1994 Data*, Contributed Paper to EPS-HEP Brussels, **eps0094**.
The 1994 data have been combined with the earlier data using a 100% correlation of the systematic errors.

[28] OPAL Collaboration, *Updated Measurement of the Tau Polarisation Asymmetry*, Contributed Paper to EPS-HEP Brussels, **eps0295**.

[29] ALEPH Collaboration, D. Buskulic *et al.*, Z. Phys. **C62** (1994) 179;
ALEPH Collaboration, *Measurement of the b forward-backward asymmetries and of the* $\bar{\chi}$ *mixing parameter using high-*p_t *leptons,* ALEPH 96-035, contributed paper to the Moriond Winter conferences, 1996;
ALEPH Collaboration, *Heavy Flavour Lepton Contribution for Summer 1994 Conferences,*

ALEPH 94-123 PHYSIC 94-107;
ALEPH Collaboration., D. Buskulic *et al.*, *Measurement of the semileptonic b branching ratios from inclusive leptons in Z decays*, Contributed Paper to EPS-HEP-95 Brussels, **eps0404**.

[30] DELPHI Collab., P.Abreu et al., Z. Phys. **C66** (1995) 323.

[31] DELPHI Collaboration, P.Abreu *et al.*, Z. Phys **C65** (1995) 569;
DELPHI Collaboration, P.Abreu *et al.*, Z. Phys **C66** (1995) 341;
DELPHI Collaboration, *Measurement of the Forward-Backward Asymmetries of* $e^+e^- \rightarrow Z \rightarrow b\bar{b}$ *and* $e^+e^- \rightarrow Z \rightarrow c\bar{c}$ Contributed Paper to EPS-HEP-95 Brussels, **eps0571**, DELPHI 95-87 PHYS 522.

[32] L3 Collaboration, O. Adriani *et al.*, Phys. Lett. **B292** (1992) 454;
L3 Collaboration, M. Acciarri *et al.*, Phys. Lett. **B335** (1994) 542;
L3 Collaboration, *Measurement of* $R_{\rm b}$ *and BR(*$\rm b \rightarrow \ell X$*) from b-quark semileptonic decays,* L3 Note 1449, July 16 1993;
L3 Collaboration, *L3 Results on* $A_{\rm FB}^{\rm b\bar{b}}$, $A_{\rm FB}^{\rm c\bar{c}}$ *and* χ *for the Glasgow Conference,* L3 Note 1624;
L3 Collaboration, *L3 Results on* $R_{\rm b}$ *and* $\rm BR(b \rightarrow \ell)$ *for the Glasgow Conference,* L3 Note 1625.
The sign of the correlation coefficient arising from the b semileptonic decay model has been corrected.

[33] OPAL Collaboration, R. Akers *et al.*, Z. Phys. **C60** (1993) 199;
OPAL Collaboration, R. Akers *et al.*, *Measurement of the Heavy Quark Forward-Backward Asymmetries and Average B Mixing Using Leptons in Multihadronic Events*, CERN-PPE/95-179.

[34] ALEPH Collaboration, D. Buskulic *et al.*, Phys. Lett. **B313** (1993) 549.

[35] L3 Collaboration, O. Adriani *et al.*, Phys. Lett. **B307** (1993) 237.

[36] ALEPH Collaboration, D. Buskulic *et al.*, Phys. Lett. **B313** (1993) 535.

[37] DELPHI Collaboration, P. Abreu et al., *Measurement of the partial decay width* $R_b = \Gamma_{b\bar{b}}/\Gamma_{had}$ *with the DELPHI detector at LEP* , CERN-PPE/96-15.

[38] OPAL Collaboration, Z. Phys. **C65** (1995) 17-30;
An Update of the Measurement of $\Gamma_{\rm b\bar{b}}/\Gamma_{\rm had}$ *using a Double Tagging Method*, Contributed Paper to EPS-HEP-95 Brussels, **eps0278**, OPAL Physics Note PN181.

[39] ALEPH Collaboration, D. Buskulic *et al.*, Phys. Lett. **B335** (1994) 99.

[40] OPAL Collaboration, R. Akers *et al.*, Z. Phys. **C67** (1995) 365.

[41] DELPHI Collaboration, *Summary of* R_c *measurements in DELPHI,* DELPHI 96-30 PHYS 604 and references therein.

[42] OPAL Collaboration, R. Akers *et al.*, Z. Phys. **C67** (1995) 27;
OPAL Collaboration, *A measurement of* $B(\rm c \rightarrow D^*)$ *and* $\Gamma_{c\bar{c}}/\Gamma_{had}$ *using a double tagging technique*, Contributed Paper to EPS-HEP-95 Brussels, **eps0289**, OPAL physics note PN 175;
OPAL Collaboration, *A summary of OPAL measurements of charm production in* Z *decays*, OPAL Physics note PN190.

[43] ALEPH Collaboration, D. Buskulic *et al.*, Z. Phys. **C62** (1994) 1;
ALEPH Collaboration, D. Buskulic *et al.*, *The Forward–Backward Asymmetry for Charm Quarks at the Z pole: an Update*, Contributed Paper to EPS-HEP-95 Brussels, **eps0634**.

[44] OPAL Collaboration, *A Measurement of the Charm and Bottom Forward-Backward Asymmetry using D Mesons with the OPAL Detector at LEP* Contributed Paper to EPS-HEP-95 Brussels, **eps0290**, OPAL Physics Note, PN183.

[45] D. Bardin *et al.*, Z. Phys. **C44** (1989) 493; Comp. Phys. Comm. **59** (1990) 303; Nucl. Phys. **B351**(1991) 1; Phys. Lett. **B255** (1991) 290 and CERN-TH 6443/92 (May 1992).

[46] A. Djouadi, B. Lampe and P.M. Zerwas, Z. Phys. **C67** (1995) 123.

[47] ALEPH Collaboration, D. Decamp *et al.*, Phys. Lett. **B259** (1991) 377.

[48] ALEPH Collaboration, ALEPH-Note 93-041 PHYSIC 93-032 (1993);
ALEPH Collaboration, ALEPH-Note 93-042 PHYSIC 93-034 (1993);
ALEPH Collaboration, ALEPH-Note 93-044 PHYSIC 93-036 (1993).

[49] ALEPH Collaboration, *Determination of* $\sin^2\theta_{\rm W}^{eff}$ *Using Jet Charge Measurements in Hadronic Z Decays* CERN PPE/96-09, Submitted to Z. Phys. C.

[50] DELPHI Collaboration, P. Abreu *et al.*, Phys. Lett. **B277** (1992) 371.

[51] DELPHI Collaboration, *Measurement of the Inclusive Charge Flow in Hadronic Z Decays,* DELPHI 96-19 PHYS 594.

[52] OPAL Collaboration, P. D. Acton *et al.*, Phys. Lett. **B294** (1992) 436.

[53] OPAL Collaboration, OPAL Physics Note PN195 (1995).

[54] T. Sjöstrand, Comp. Phys. Comm. **82** (1994) 74.

[55] G. Marchesini *et al.*, Comp. Phys. Comm. **67** (1992) 465.

[56] CHARM II Collaboration, P. Vilain *et al.*, Phys. Lett. **B335** (1994) 246.

[57] S. Bethke, Proceedings of the QCD '94 Conference, Montpellier, France, Nucl. Phys. B. (Proc. Suppl.) **39B,C** (1995) 198.

[58] *Reports of the working group on precision calculations for the Z resonance*, eds. D. Bardin, W. Hollik and G. Passarino, CERN Yellow Report 95-03, Geneva, 31 March 1995.

[59] Electroweak libraries:
ZFITTER: see Reference 45;
BHM: G. Burgers, W. Hollik and M. Martinez; M. Consoli, W. Hollik and F. Jegerlehner: Proceedings of the Workshop on Z physics at LEP I, CERN Report 89-08 Vol.I,7 and G. Burgers, F. Jegerlehner, B. Kniehl and J. Kühn: the same proceedings, CERN Report 89-08 Vol.I, 55.
These computer codes have recently been upgraded by including the results of [58] and references therein.

[60] T. Hebbeker, M. Martinez, G. Passarino and G. Quast, Phys. Lett. **B331** (1994) 165.

[61] M. L. Swartz, *Reevaluation of the Hadronic Contribution to* $\alpha(M_Z^2)$, SLAC-PUB-6710, November 1994, SLAC-PUB-95-7001, September 1995.

[62] A.D. Martin and D. Zeppenfeld, Phys. Lett. **B345** (1994) 558.

[63] S. Eidelmann and F. Jegerlehner, Z. Phys. **C67** (1995) 585.

[64] H. Burkhardt and B. Pietrzyk, Phys. Lett. **B356** (1995) 398.

[65] The average for m_W has been obtained taking into account the measurements [12–15]. The method of the combination follows the description in [67] treating the uncertainty due to parton distribution functions as the only common error. The measurements are averaged weighted by their uncorrelated uncertainties.

[66] A. Blondel and C. Verzegnassi, Phys. Lett. **B311** (1993) 346.

[67] M. Demarteau *et al.*, *Combining W Mass Measurements*, CDF/PHYS/CDF/PUBLIC/2552 and DØ NOTE 2115.